


 Cite this: *RSC Adv.*, 2020, **10**, 28918

Synthesis of novel liquid crystalline and fire retardant molecules based on six-armed cyclotriphosphazene core containing Schiff base and amide linking units[†]

 Zuhair Jamain,^a Melati Khairuddean^{*b} and Tay Guan-Seng^c

Nucleophilic substitution reaction between 4-hydroxybenzaldehyde and hexachlorocyclotriphosphazene, HCCP formed hexakis(4-formlyphenoxy)cyclotriphosphazene, **1**. Intermediates **2a–e** was formed from the alkylation reaction of methyl 4-hydroxybenzoate with alkyl bromide which further reduced to form benzoic acid intermediates. Further reaction of **2a–e** and other substituted benzoic acid formed **3a–h**, which then reduced to give subsequent amines, **4a–h**. Other similar reaction was used to synthesis **4i**. Condensation reaction between **1** and **4a–i** yielded hexasubstituted cyclotriphosphazene compounds, **5a–i** having Schiff base and amide linking units, and these compounds consist of different terminal substituents such as heptyl, nonyl, decyl, dodecyl, tetradecyl, hydroxy, carboxy, chloro, and nitro groups, respectively. Compound **5j** with amino substituent at terminal end was formed from the reduction of **5i**. All the intermediates and compounds were characterized using Fourier Transform Infrared (FT-IR), Nuclear Magnetic Resonance (NMR) and CHN elemental analysis. Mesophase texture of these compounds were determined using Polarized Optical Microscope (POM) and their mesophase transition were further confirmed using Differential Scanning Calorimetry (DSC). Only compounds **5a–e** with alkoxy chains exhibited smectic A phase while other intermediates (**1**, **2a–e**, **3a–h**, and **4a–i**) and final compounds (**5f–j**) are found to be non-mesogenic with no liquid crystal behaviour. The confirmation of the identity of the SmA phase was determined using XRD analysis. The study on the structure–properties relationship was conducted in order to determine the effect of the terminal group, length of the chains and linking units to the mesophase behaviour of the compounds. Moreover, the fire retardant properties of these compounds were determined using Limiting Oxygen Index (LOI) testing. Polyester resin with LOI value of 22.53% was used as matrix for moulding in the study. The LOI value increased to 24.71% when this polyester resin incorporated with 1 wt% of HCCP. Generally, all the final compounds showed a positive results with LOI value above 27% and the highest LOI value was belonged to compound **5i** with 28.53%. The high thermal stability of the Schiff base molecules and the electron withdrawing group of the amide bonds and nitro group enhanced the fire retardant properties of this compound.

 Received 28th April 2020
 Accepted 23rd July 2020

 DOI: 10.1039/d0ra03812a
rsc.li/rsc-advances

1. Introduction

In the early years, Allcock and his co-workers started the research work on phosphazene compounds which was then developed into the investigation of phosphazene liquid crystalline materials.^{1,2} Hexachlorocyclotriphosphazene, **HCCP** ($\text{N}_3\text{P}_3\text{Cl}_6$) is a ring consisting of alternating phosphorus and

nitrogen atoms, whereby six chlorine atoms can be substituted with any selected nucleophiles. Due to the high reactivity of the P–Cl bond, the corresponding substitution method allows the structure–activity studies in the side arm and their multiarmed rigid ring allows the exploration of the discotic structures.³ It was reported that compounds with the cyclotriphosphazene core (N_3P_3) attached to different substrates exhibited different physical and chemical properties.⁴ They have been used in many fields such as liquid crystal and fire retardant applications due to their fascinating properties.^{5,6}

Liquid crystal (LC) is an anisotropic material with flowing properties (liquid) as well as ordered (solid) and optical properties.⁷ Since it has the features of both fluid and solid, it became an important intermediate phase or mesomorphic phase.⁸ LC of organic compounds is divided into two categories

^aFaculty of Science and Natural Resources, Universiti Malaysia Sabah (UMS), 88400 Kota Kinabalu, Sabah, Malaysia. E-mail: zuhairjamain@ums.edu.my

^bSchool of Chemical Sciences, Universiti Sains Malaysia (USM), 11800 Penang, Malaysia. E-mail: melati@usm.my

^cSchool of Industrial Technology, Universiti Sains Malaysia (USM), 11800 Penang, Malaysia

[†] Electronic supplementary information (ESI) available: Fig. 1–5: DSC thermogram of compounds **5a–e**, respectively. See DOI: 10.1039/d0ra03812a



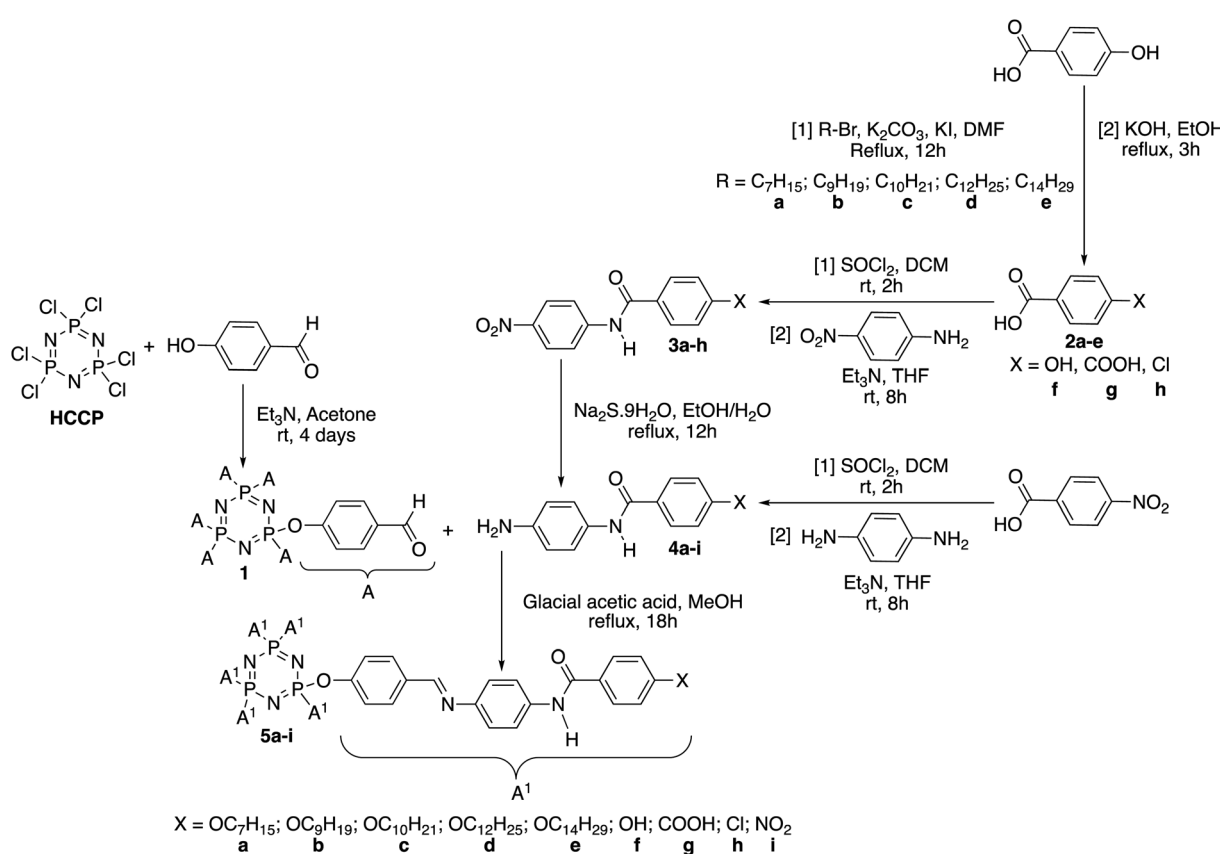
which are lyotropic and thermotropic LC. Thermotropic LC are influenced by the change in temperature while lyotropic LC which are composed mainly of the amphiphilic bilayer are concentration and temperature dependant.^{9,10}

The influence of different elements and the extended chemical subunits on the molecules allows the construction of the targeted liquid crystal compounds. The molecular shape and the terminal chain length are the key variables in designing new liquid crystal compounds with specific types of molecular organization in a particular range of temperature.^{11–13} Linking units are normally structural units that connect one core to another, which maintain the linearity of the core while being compatible with the rest of the structure. A linking unit between ring systems is to increase the length of the molecules and to alter the polarisability and flexibility of the molecules.¹⁴ Schiff base is one the interesting linking unit that provide a stepped core structure which can maintain the linearity of the molecules to provide high stability. This enables the mesophase formation whereby the phase transition temperature and the physical properties changes are usually contributed by the linking group.¹⁵ On the other hand, the formation of an amide linking unit led to higher rigidity due to the presence of the partial double bond character of the C–N bond which resulted in higher transition and clearing temperatures of the mesogens.¹⁶ The partial double bond in C–N bond reduces the coplanarity of the molecule and the broadening of the rigid core, which

resulted in the molecules that favoured a lamellar arrangement in the smectic layer.¹⁷ The correlation between the molecular structure such as core system, linking units and terminal groups are the most important aspect in liquid crystal field.

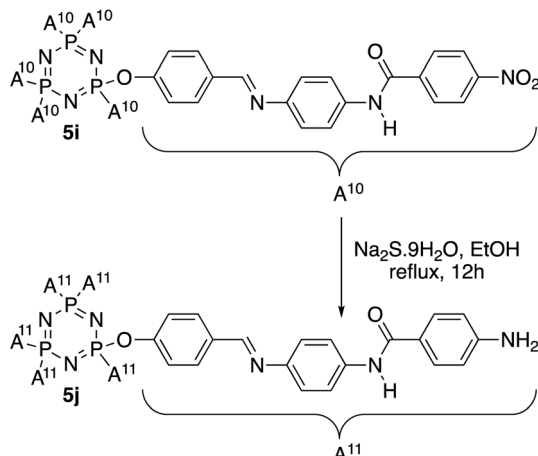
Jiménez *et al.* (2011) reported the synthesis of hexasubstituted cyclotriphosphazene derivatives attached to the side arms with an ester linking unit but different terminal chains. The formation of the mesophase depended on the balance between the rigid core and the flexible terminal chains while the type and stability of the mesophase were determined by the space filling and nanosegregation. The combination of these factors along with tailoring of the interface curvature by the space requirements of the incompatible molecular blocks will determines the difference mesophase morphologies of these cyclotriphosphazene molecules.¹⁸ Moreover, He *et al.* (2013) have synthesized the room temperature columnar mesogens of hexasubstituted cyclotriphosphazenes compounds with Schiff base and ether linking units. They found out that increasing the chain length increased the melting point and decreased the clearing point.¹⁹

On the other side, HCCP also known to be used as a molecule to have high fire retardancy. Fire retardant materials play an important role in protecting property from damage. Fire retardation occurred due to the removal of heat from the materials that can burn and the formation of char during the fire which will interrupt the contact from combustion.²⁰ Generally,



Scheme 1 Formation of intermediates (1, 2a–e, 3a–h, and 4a–i) and hexasubstituted cyclotriphosphazene compounds, 5a–i.





Scheme 2 Reduction of compound 5i to 5j.

materials with limiting oxygen index (LOI) value above 26% are considered fire retardant and self-extinguishing behaviour can be observed.^{21,22} Zhang *et al.* (2012) have synthesized and studied the fire retardant properties of hexakis(4-nitrophenoxy) cyclotriphosphazene on poly(ethylene terephthalate). The LOI value of poly(ethylene terephthalate) increased from 26.8% to 35.1% when 10 wt% of this compound was added.²³ Moreover, Rong *et al.* have conducted two independent studies on the cyclotriphosphazene core system in 2015 and 2017. Their

findings showed that the modification of cyclotriphosphazene core system able to induce the thermal stability, which enhances the fire resistance of the compounds.^{24,25}

Therefore, the interest of the research is to gain a better insight of the structure–properties relationship of these types of compounds. Addition of **HCCP** into a compound is to increase the resistance of the material towards ignition. Both liquid crystal and fire retardant properties were studied. Thus, this research focused on the preparation of a series of hexasubstituted cyclotriphosphazene derivatives with Schiff base and amide linking units that bore a different terminal end. In this work, polyester resin will be used as a medium for moulding in order to study the fire retardant of the compounds. Only 1 wt% is added in this resin in order to achieve highest fire retardancy with less additive usage. Polyester resin is chosen due to good mechanical properties, fast curing, low cost and more sensitive to elevated temperatures.

2. Results and discussion

In this work, **HCCP** has been used as a core system to prepare hexasubstituted cyclotriphosphazene compounds consist of Schiff base and amide linking units. Intermediate **1** was synthesized from the reaction of **HCCP** with 4-hydroxybenzaldehyde. Methyl 4-hydroxybenzoate with different alkyl bromide (heptyl, nonyl, decyl, dodecyl, and tetradecyl) were used to form methyl 4-(alkoxy)benzoates. Without isolation,

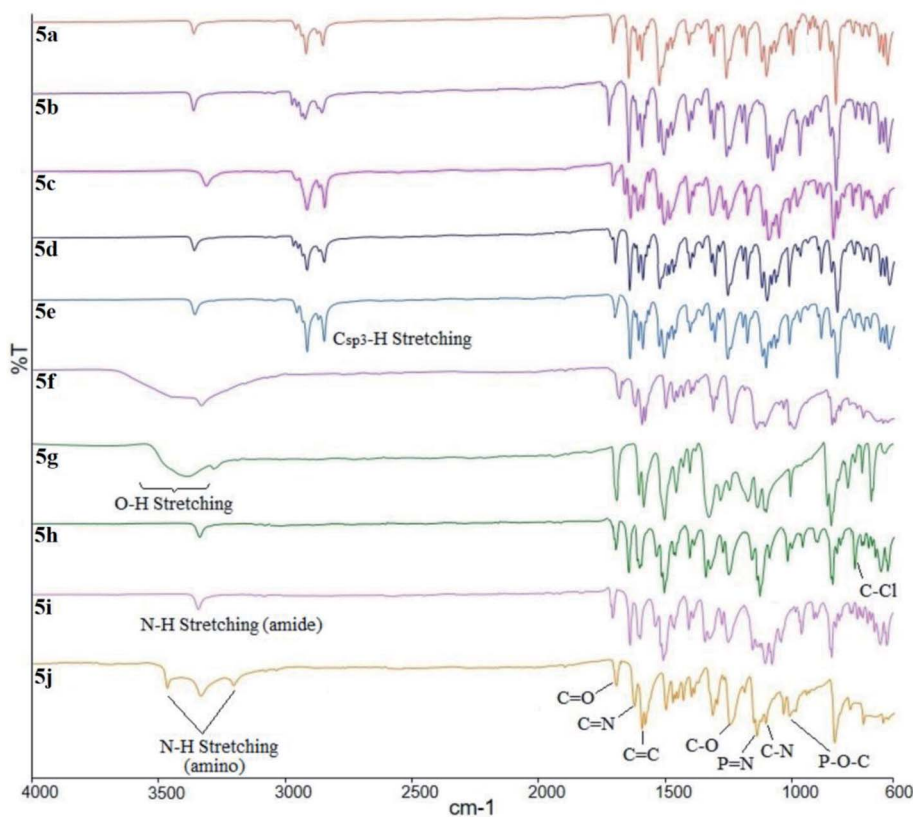


Fig. 1 FTIR spectra overlay of compounds 5a–j.



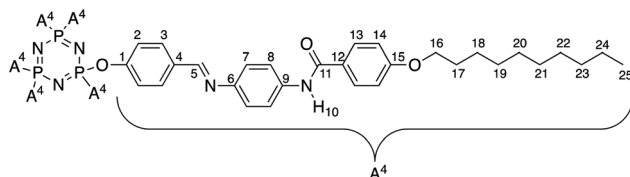


Fig. 2 Structure of compound 5c with complete atomic numbering.

these methyl 4-(alkoxy)benzoates were further reduced to form subsequent benzoic acid intermediates, **2a–e**. Intermediates **3a–h** with amide linking unit were afforded from the reaction of **2a–e** and some *para* substituted benzoic acid such as hydroxy, carboxy, and chloro, respectively. These intermediates were then reduced to form **4a–h**. Intermediate **4i** was prepared using different synthetic route. Finally, condensation reaction of **1** with **4a–i** yielded final compounds **5a–i** with Schiff base and amide linking units. Further reduction of **5i** formed compound **5j** with amino group at the terminal end. The structures of these intermediates and final compounds were confirmed using FTIR, NMR and CHN elemental analysis. The overall synthesis pathway for intermediates and hexa-substituted cyclophosphazene compounds for this series are described in Schemes 1 and 2.

2.1. FTIR spectral data discussion

Intermediate **1** was successfully synthesized with the disappearance absorption band at 3250 cm^{-1} for O-H stretching. The other absorption bands were observed at 2730 ($\text{H}-\text{C}(\text{O})\text{O}(\text{H}-\text{C}=\text{O})$), 1700 ($\text{C}=\text{O}$), 1595 ($\text{C}=\text{C}$), and 1205 cm^{-1} ($\text{C}-\text{O}$). The IR data of intermediates **2a–e** showed the absorption bands at 3250 (O-H stretching), 2852 and 2921 ($\text{Csp}^3\text{-H}$ stretching), 1680 ($\text{C}=\text{O}$ stretching), 1605 ($\text{C}=\text{C}$ stretching), and 1250 cm^{-1} ($\text{C}-\text{O}$ stretching). Intermediates **3a–h** were successfully synthesized as evident from the appearance of a new band at 3300 cm^{-1} (N-H stretching) of the amide linkage. Further reduction of intermediates **3a–h** gave rise to intermediates **4a–h** with the appearance of two absorption bands at 3200 and 3400 cm^{-1} (N-

H stretching) in the IR spectra of the latter. Intermediate **4i** which was synthesized using other method also showed similar bands at 3207 and 3408 cm^{-1} (N-H stretching). Other bands at 1690 ($\text{C}=\text{O}$), 1590 ($\text{C}=\text{C}$), 1250 ($\text{C}-\text{O}$), and 1175 cm^{-1} ($\text{C}-\text{N}$) stretching were observed in both intermediates **3a–h** and **4a–i**. The diagnostic bands at 3200 and 825 cm^{-1} were attributable to the O-H stretching and C-Cl bending, respectively in **3f–g** and **4f–g**.

The overlay IR spectra of compounds **5a–j** with Schiff base and amide linking units are shown in Fig. 1. The reaction between hexa-substituted cyclophosphazene benzaldehyde, **1** and intermediates **4a–i** gave **5a–i**. The appearance of the expected absorption band at 1644 cm^{-1} for C=N stretching confirmed the successful condensation reaction of intermediates **4a–i**. Further reduction of compound **5i** produced compound **5j** with the appearance of two-spike at 3207 and 3416 cm^{-1} (N-H stretching). Besides, all the compounds showed the absorption band for the N-H stretching of the amide linkage at 3365 cm^{-1} .

On the other hand, compounds **5f** and **5g** showed the overlapping of the absorption bands for hydroxy (-OH) and N-H stretching of the amide groups because peak broadening of the O-H stretching. Other absorptions bands were observed at 1691 cm^{-1} for the carbonyl ($\text{C}=\text{O}$) stretching, and also at 1592 , 1254 , and 1178 cm^{-1} for $\text{C}=\text{C}$, $\text{C}-\text{O}$, and $\text{C}-\text{N}$ stretching, respectively. As usual, the diagnostic bands at 2851 and 2919 cm^{-1} which corresponding to the $\text{Csp}^3\text{-H}$ symmetrical and asymmetrical stretching of alkoxy chains can be observed in compounds **5a–e**. In addition, the bending at 819 cm^{-1} was assigned to the C-Cl bending in compound **5h**. The absorption bands from the cyclophosphazene ring, $\text{P}=\text{N}$ stretching appeared at 1197 cm^{-1} , while $\text{P}-\text{O}-\text{C}$ bending was located at 977 cm^{-1} .

2.2. NMR spectral data discussion

The absent of the hydroxyl signal in the $^1\text{H-NMR}$ spectrum of intermediate **1** confirmed the nucleophilic substitution of the 4-hydroxybenzaldehyde. The singlet at $\delta 9.90\text{ ppm}$ was assigned to

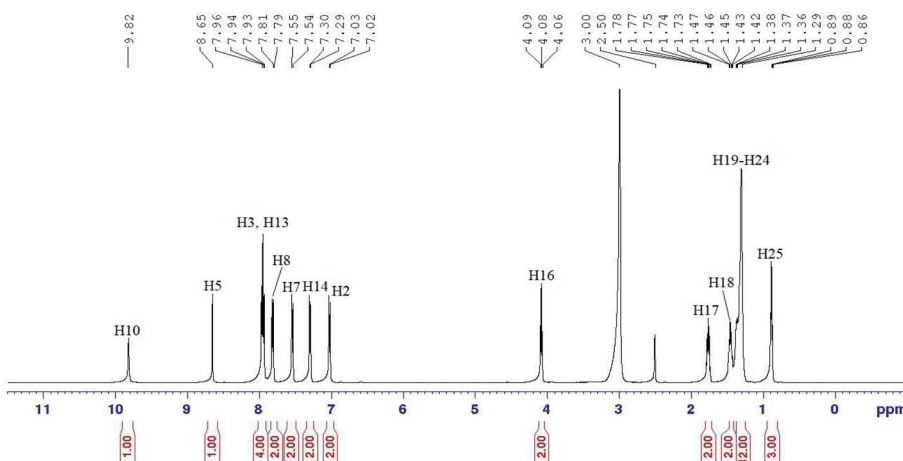


Fig. 3 ^1H NMR spectrum of compound 5c.





the aldehydic proton and two doublets at δ 7.78 and 7.16 ppm were assigned for two different aromatic protons in the compound. The ^{13}C -NMR data of **1** showed the signal for aldehydic carbon at δ 191.69 ppm and four aromatic signals at δ 153.59, 133.55, 131.46, and 121.03 ppm. The ^{31}P NMR showed a singlet at δ 7.60 ppm, indicated that all the benzaldehyde was successfully attached to the phosphorus atom in the cyclo-triphosphazene ring.

The ^1H -NMR data of **2a–e** revealed similar pattern with two doublets assigned for two aromatic protons, while all the peaks in the upfield region were assigned to the aliphatic protons of heptyl, nonyl, decyl, dodecyl, and tetradecyl chains. The ^{13}C -

NMR data of **2a–e** showed the carbon signals for aromatic ring and aliphatic chains. The signal for the aliphatic carbons displayed similar pattern but only differed in the intensity, which due to the different length in the carbon chains. The carboxy carbon for **2a–e** showed a signal at the most downfield region at δ 168.78, 169.36, 168.78, 167.95, and 169.18 ppm, respectively. No signal for the methyl observed in both spectra indicating that the reduction reaction was a success.

Meanwhile, the ^1H -NMR data of intermediates **3a–h** showed a similar pattern with a singlet corresponded to the amide proton (N-H) in the most downfield region at δ 10.61, 10.22, 10.33, 10.25, 10.25, 9.72, 11.06, and 9.90 ppm, respectively. Both

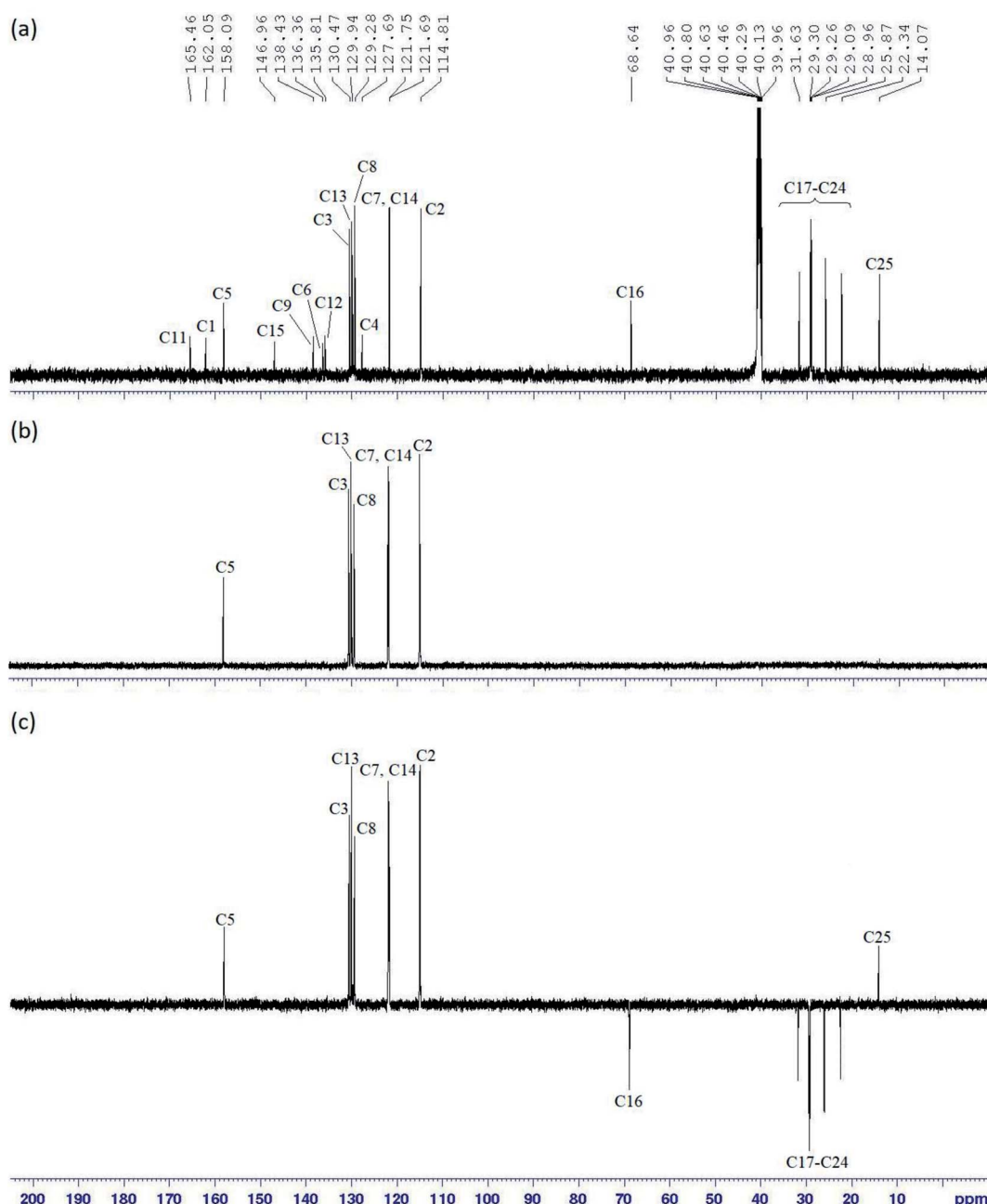


Fig. 4 (a) ^{13}C NMR, (b) DEPT 90 and (c) DEPT 135 spectra of compound **5c**.

the ^1H and ^{13}C -NMR data showed the presence of four doublets of protons and eight carbons signal for the aromatic ring. The reduction of intermediates **3a–h** to **4a–h** showed the appearance of N–H signals of the amine group at δ 5.00 ppm in the ^1H -NMR spectra. For final compound, **5c** was used to represent the structure confirmation in the series. The structure of compound **5c** with complete atomic numbering is illustrated in Fig. 2.

In the ^1H NMR spectrum of compound **5c** (Fig. 3), two singlets in the downfield region at δ 9.82 (H5) and δ 8.65 ppm (H10) were assigned to the amide and azomethine protons, respectively. Five distinguishable doublets located within δ 7.02–7.96 ppm were assigned to the aromatic protons. One of these signals with integrating to four protons were overlapped and appeared as a triplet (H3 and H13).

However, the effect of the amide group as an electron withdrawing group which caused the electron density of the molecule to decrease, forced H8 to experience more deshielding effect compared to H7 and H14, which was more deshielded than H2. An oxymethylene proton, H16 appeared as a triplet at δ 4.08 ppm and all the methylene protons (H17–H24) were assigned in the region of δ 1.27–1.78 ppm. A triplet in the most upfield region was assigned to H25 at δ 0.88 ppm.

The ^{13}C NMR spectrum of compound **5c** (Fig. 4a) showed 23 carbon signals comprising of one azomethine, seven

quaternary, six aromatics, one oxymethylene, seven methylene, and one methyl carbons. DEPT 90 (Fig. 4b) and DEPT 135 (Fig. 4c) experiments were conducted to distinguish the types of carbons. In the DEPT 90 spectrum, the azomethine carbon, C5 was observed at δ 158.09 ppm while the aromatic carbons resonated at δ 130.47 (C3), 129.94 (C13), 129.28 (C8), 121.75 (C7), 121.69 (C14), and 114.81 ppm (C2).

For others homologues, the ^1H and ^{13}C NMR spectra of compounds **5a**, **5b**, **5d**, and **5e** appeared a similar splitting patterns and chemical shifts as shown in compound **5c** but only differed in term of the number of protons and carbons in the alkyl chains. Compounds **5f–j** attached with small substituents such as hydroxy, carboxy, chloro, nitro, and amino at the terminal end showed a singlet of amide signal and six doublets for aromatic protons in the ^1H NMR spectra.

Both ^1H and ^{13}C NMR spectra of these compounds showed a slight difference in the chemical shift values, which due to the chemical environment, electronegativity effect, and bond angles. Meanwhile, compounds **5f** and **5g** displayed an additional signal for hydroxyl and carboxyl proton peaks in the ^1H NMR spectra. Moreover, all the compounds in this series showed a singlet in the ^{31}P NMR spectrum due to hexa-substituted in the arms (Fig. 5).

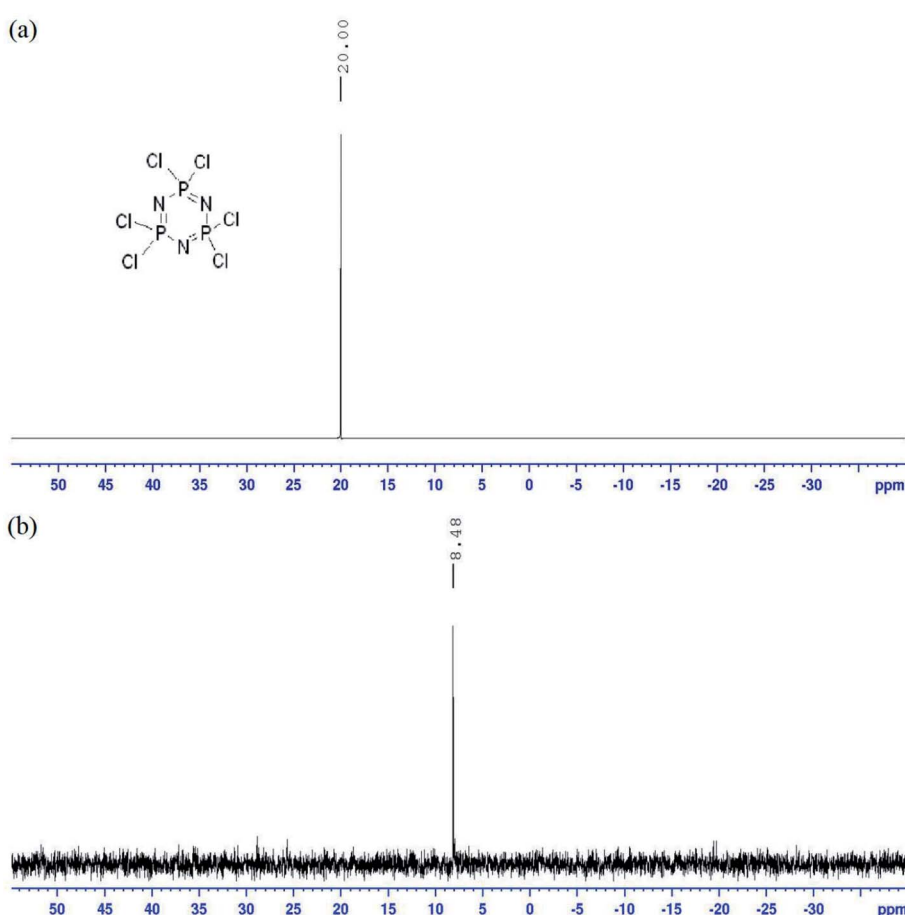


Fig. 5 ^{31}P NMR spectrum of compound **5c**.



2.3. Determination of liquid crystal behaviour using POM

The POM optical photomicrograph was obtained using the Olympus system model bx53 linksys32. In this study, only compounds **5a–e** with Schiff base and amide linking unit attached to different chain length at the terminal end were

found to be mesogenic. These compounds showed Smectic A (SmA) phase of focal-conic fans in both heating and cooling cycles (Fig. 6). However, other intermediates and compounds did not show any liquid crystal texture, therefore these compounds are known as non-mesogenic. Observation under POM for compounds **5f–j** only showed the phase transition of

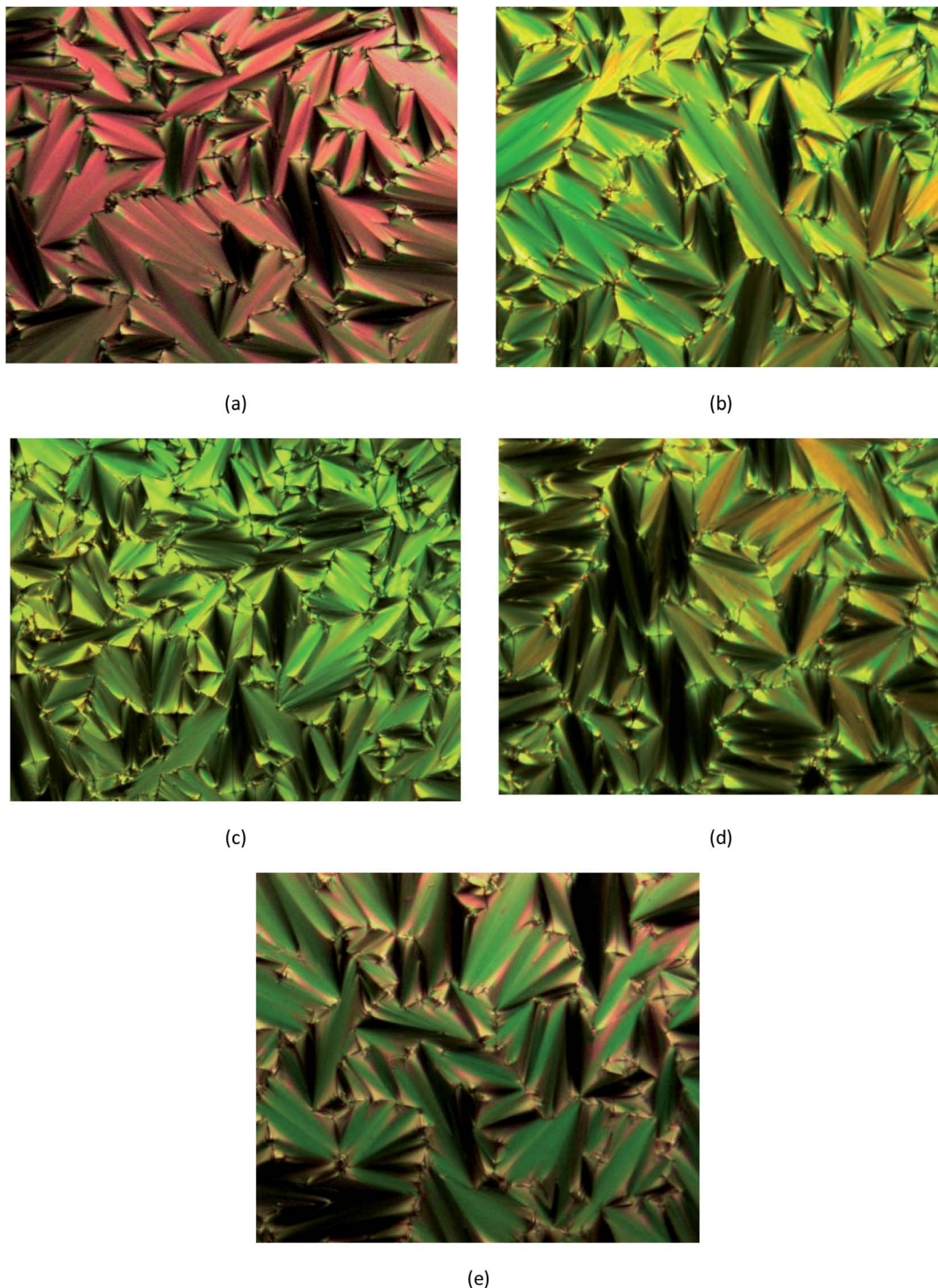


Fig. 6 The optical photomicrographs of compounds **5a–e** in the cooling cycle showing the SmA phase, (a) 270.55 °C for compound **5a**, (b) 268.77 °C for compound **5b**, (c) 268.50 °C for compound **5c**, (d) 255.43 °C for compound **5d**, and (e) 247.78 °C for compound **5e** (magnification scale: 20 × 0.25).



Table 1 Phase transitional properties of compounds **5a–e** upon heating and cooling cycles^a

Compound	Mode	Transition temperature (°C), enthalpy, ΔH (kJ mol ⁻¹)
5a	Heating	Cr 188.02, 186.54 SmA 286.83, 48.13 I
	Cooling	I 280.47, -58.43 SmA 170.05, -212.30 Cr
5b	Heating	Cr 177.09, 173.10 SmA 287.87, 68.64 I
	Cooling	I 282.57, -73.98 SmA 161.53, -207.61 Cr
5c	Heating	Cr 174.44, 156.52 SmA 286.15, 70.96 I
	Cooling	I 278.75, -77.83 SmA 158.16, -204.07 Cr
5d	Heating	Cr 171.44, 191.73 SmA 281.61, 83.37 I
	Cooling	I 275.76, -88.98 SmA 155.73, -211.63 Cr
5e	Heating	Cr 168.58, 125.75 SmA 276.25, 76.22 I
	Cooling	I 267.13, -76.78 SmA 149.00, -182.89 Cr

^a Cr = crystal, SmA = smectic A, I = isotropic.

crystal to isotropic in the heating cycle. Similar phase transitions were also observed in the reversed order of the cooling cycle.

2.4. Determination of thermal transitions using POM

The DSC experiment was conducted to confirm the phase transition observed under POM. Only compounds with liquid crystal were further sent for DSC measurement. The transition temperatures and enthalpy change involved during the transition in the heating and cooling cycles were recorded in the DSC

thermogram. The thermal enthalpy, ΔH (kJ mol⁻¹) of each phase transition of compounds **5a–e** are summarized in Table 1.

The DSC thermograms of compounds **5a–e** showed two curves for the transition of crystal to SmA and to isotropic phase in both cycles. All compounds showed high melting and clearing temperature in the heating cycle. From the DSC data, the melting temperature was observed at 188.02, 177.09, 174.44, 171.44, and 168.58 °C, which corresponded to compounds **5a–e**, respectively. The DSC thermogram of compound **5c** was illustrated in Fig. 7. The melting and clearing temperature of the compounds showed similar pattern whereby the temperature decreased as the number of alkyl chains increased. As reported by Moriya *et al.* (2006), the melting and clearing temperature decreased with an increased number of alkyl chains.²⁶ Moreover, all the compounds have high enthalpy changes at the clearing temperature. This behaviour was related to the high molecular weight of hexasubstituted cyclotriphosphazene

Table 2 The XRD data of compounds **5c**

XRD data analysis	Value
2 theta	1.93
<i>d</i> -Layer spacing	45.74
Molecular length (<i>L</i>)	41.23
Calculated <i>d/L</i>	1.11
Arrangement of SmA	Monolayer

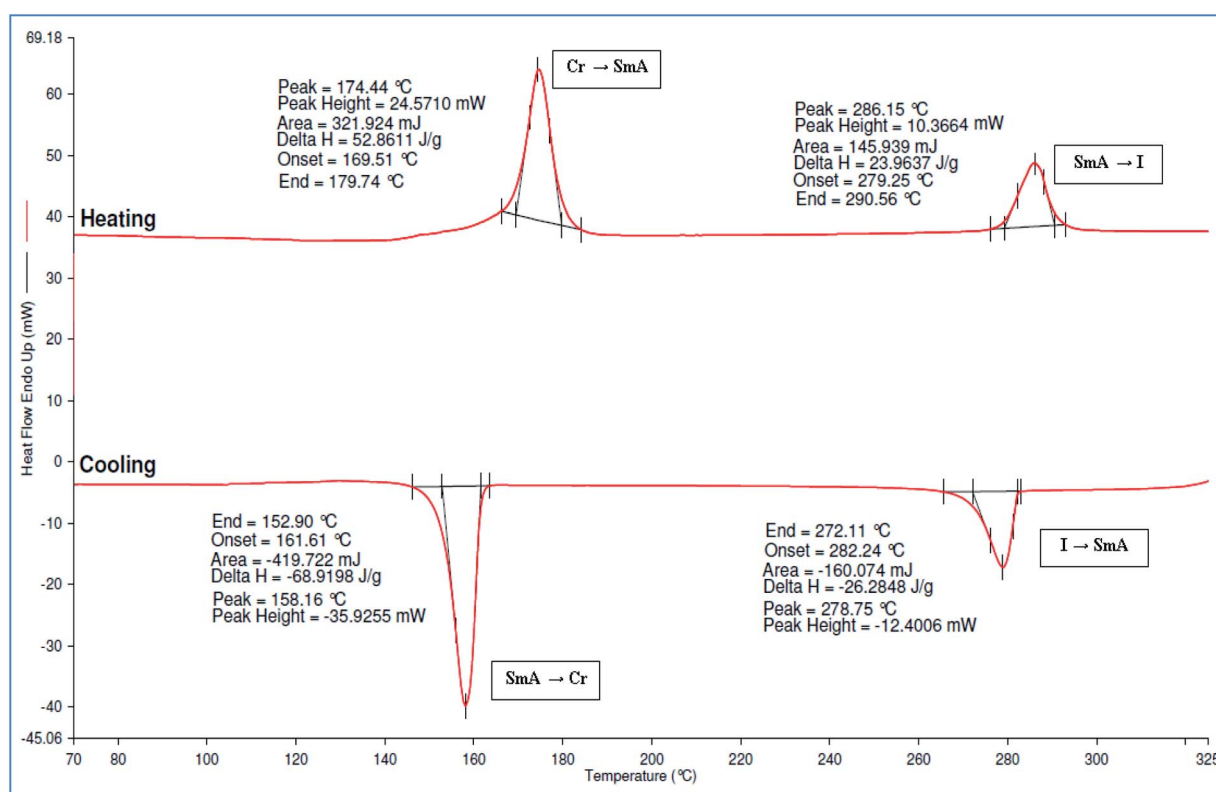


Fig. 7 DSC thermogram of compound **5c**.



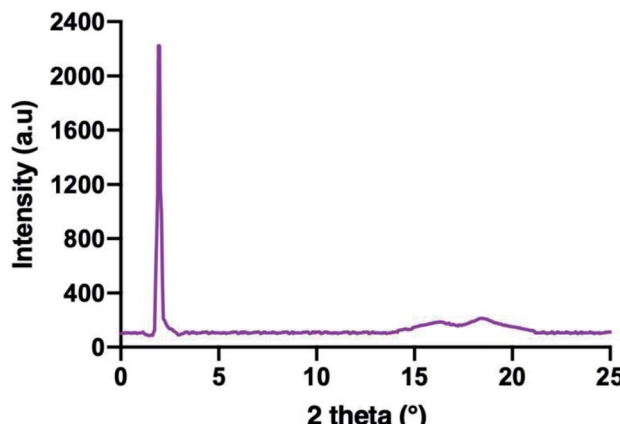


Fig. 8 XRD diffractogram of compound 5c.

compounds, which effected by their π -energy, hydrogen-bonding and van der Waals forces.²⁷

2.5. Determination of liquid crystal using XRD analysis

The confirmation of the SmA phase observed in these series were carried out using XRD analysis. The XRD data of compounds **5c** is summarized in Table 2. Compound **5c** was used as representative for further discussion. The XRD diffractogram of compound **5c** is shown in Fig. 8. The XRD diffractogram of compound **5c** showed a single sharp peak at $2\theta = 1.19^\circ$ and a broad peak with wide angle at $2\theta = 15\text{--}21^\circ$, indicating that the molecules favour the smectic layered arrangement.²⁸ Generally, compound exhibited the lamellar structure for smectic liquid crystalline phase showed the sharp and strong peak at low angle ($1^\circ < 2\theta < 4^\circ$), and a broad peak associated with lateral packing at $2\theta \approx 20^\circ$ in the XRD curve.²⁹ The sharp peak indicated the regular arrangement in spaced layer, while a broad peak for the disordered packing of alkyl chains.³⁰ According to the XRD data, the *d*-layer spacing and molecular length (*L*) obtained from the molecular calculation of compound **5c** was found to be 45.74 Å and 41.23 Å, respectively. The calculated *d/L* was 1.11 (*d* \approx *L*), which approximately to 1. This phenomenon showing that the SmA phase observed under POM is monolayer arrangement. This suggested that the side arms which connected to the phosphorus atoms of the cyclotriphosphazene ring were arranged three up and three down. The behaviour of homeotropic alignment caused these side arms aligns perpendicular to the cyclotriphosphazene ring as this shape is suitable for the smectic arrangement.³⁰ The proposed molecular shape and the possible smectic arrangement of compound **5c** are shown in Fig. 9.

2.6. Structure–properties relationship

The skeleton structures of a molecule influence the liquid crystal properties. A compound must possess certain requirement in order to exhibit liquid crystal mesophase. The physical properties of even the simplest liquid crystal compound are truly remarkable due to the self-assembly of molecules in an ordered, yet fluid, and liquid crystal mesophase.

The main criteria for a molecule to adopt liquid crystal behaviour include the molecular shape which should be relatively thin or flat within rigid molecular frameworks, which usually based on benzene rings.³¹ In general, terminal group which extends the molecular long axis without increasing the molecular width increase the thermal stability of the mesophase. The nature of the terminal substituents or end groups in the molecule of the mesogen has profound influence on the liquid crystal properties of the compound. There are varieties of terminal groups being employed in the liquid crystal molecules and the common groups vary from a small polar substituent (*e.g.* chloro or nitro) to a long chain (*e.g.* alkyl or alkoxy).³² The choice of a terminal group is very important to generate the expected liquid crystal mesophase in a molecule.

Most of the molecules consist of one terminal alkyl chain showed liquid crystal behaviour. This was proven when all the final compounds (**5a–e**) with the alkoxy chains at the terminal end exhibited the smectic A phase in both cooling and heating cycles. The length of the alkoxy side chain showed strong influence on the mesophase formation.³³ Longer alkoxy chains induced the liquid crystal behaviour with broader temperature ranges as well as decreased melting temperatures, T_m .³⁴ In addition, the number of alkoxy side chains greatly affect molecular self-assembly.³⁵ Besides, the long alkyl chains add flexibility to the rigid core and stabilize the molecular interactions needed for the formation of liquid crystal mesophase.³⁴

Conjugation within the Schiff base moiety led to possible of controlling the alignment and orientation of their molecules to generate liquid crystal properties.³⁶ Schiff base linking unit provide a stepped core structure which can maintain the molecular linearity.³² This linearity provides high stability and enabling mesophase formation. However, all compounds (**5f–j**) with small substituent such as hydroxy, carboxy, chloro, nitro, and amino groups at the terminal end were found to be non-mesogenic. Kelker and Hatz reported the behaviour of the small substituent at the terminal end do not always form liquid crystal phases.^{33,35} The lone pair of electrons or π bonds in compounds **5f** and **5g** tend to resonate onto the aromatic ring which resulted in the cancellation of dipole moments of the molecules.^{36,37} As a result, the formation of the mesophase in the molecules cannot be induced.

Even though compound **5h** and **5i** attached with polar substituent, which possesses strong dipole moment, the presence of the amide linking unit resulted in high melting temperature and the mesophase cannot be observed.¹⁶ Compound **5j** did not exhibited any liquid crystal character due to the properties of the NH_2 as an electron donating group, which maximise the repulsive interactions between adjacent aromatic rings and caused the tendency for formation of the mesophase was reduced.³⁸ The POM observation of compounds **5a–j** are summarized in Table 3.

2.7. Determination of fire retardant properties using LOI testing

In this research, polyester resin has been used as a matrix for moulding. Polyester resins are unsaturated synthetic resin and



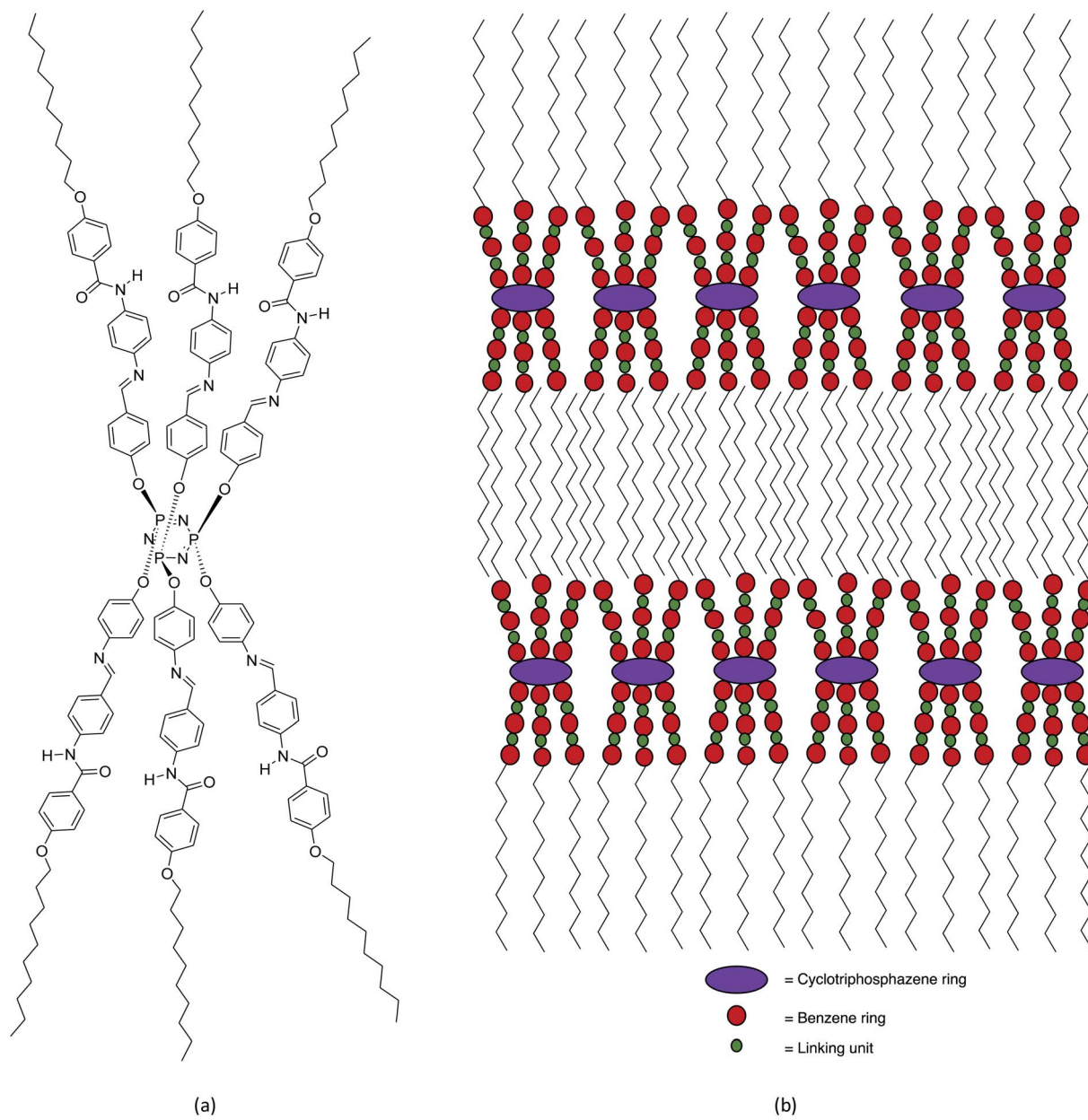


Fig. 9 (a) The proposed molecular shape and (b) the possible smectic arrangement of compound 5c.

Table 3 POM observation of compounds 5a–j

Compound	Terminal substituent	POM observation
5a	Heptyloxy	(-OC ₇ H ₁₅)
5b	Nonyloxy	(-OC ₉ H ₁₉)
5c	Decyloxy	(-OC ₁₀ H ₂₁)
5d	Dodecyloxy	(-OC ₁₂ H ₂₅)
5e	Tetradecyl	(-OC ₁₄ H ₂₉)
5f	Hydroxy	(-OH)
5g	Carboxy	(-COOH)
5h	Chloro	(-Cl)
5i	Nitro	(-NO ₂)
5j	Amino	(-NH ₂)

can be considered as a combustible material. This resin produces a lot of heat during combustion due to low thermal stability and becomes a potential to fire risk. Thus, the modification of polyester resin by mixing with hexasubstituted cyclotriphosphazene compounds having fire retardant properties are needed to overcome this problem.

The sample was prepared by mixing 1 wt% of the final compound with polyester resin. About 1 wt% of methyl ethyl ketone peroxide (MEKP) curing agent was added to the mixture and stirred until the sample is homogeneous and then poured into the moulds. The samples were cured for 5 hours in an oven at 60 °C and left overnight at room temperature before it was burned using LOI testing. The LOI test was performed using an



Table 4 LOI test results

Material	LOI value (%)
Pure polyester resin	22.53 (±0.00)
Polyester resin + 1 wt% of HCCP	24.71 (±0.00)
Compound 5a	27.90 (±0.00)
Compound 5b	27.71 (±0.00)
Compound 5c	27.71 (±0.00)
Compound 5d	27.55 (±0.00)
Compound 5e	27.53 (±0.00)
Compound 5f	28.37 (±0.00)
Compound 5g	27.93 (±0.04)
Compound 5h	28.42 (±0.00)
Compound 5i	28.53 (±0.00)
Compound 5j	27.90 (±0.00)

FTT oxygen index, according to BS 2782: Part 1: Method 141 and ISO 4589 with the dimension of 120 mm × 10 mm × 4 mm.

According to LOI data in Table 4, pure polyester resin has the LOI value of 22.53%. The LOI value of polyester resin was increased to 24.71% when incorporated with 1 wt% of **HCCP**. Schiff base linking units was found to enhance the properties of fire-retardant. This phenomenon was attributed to the high thermal stability of the Schiff base molecules, which promoted the formation of char on the surface in the condensed phase.³⁹ Interestingly, when Schiff base unit was combined with an amide unit, the LOI values showed a slight increase. This positive result was attributed to the properties of the electron withdrawing group of the amide bond which enhanced the flammability properties of the compounds.^{40,41} As a result, all the compounds have high LOI value, indicating these compounds have high thermal stability and fire retardancy. Compound **5i** showed the highest LOI value compared to other compounds due to the effect of electron withdrawing of nitro group which enhance the synergistic effect of P–N bonds.⁴² This behaviour caused the compounds exhibited both condensed and gas phase action and thus, prevents the sample from further burning. Hence, these compounds possessed highest LOI value.

3. Experimental

3.1. Chemicals

The chemicals and solvents used in this work are phosphonitrilic chloride trimer, 1-bromoheptane, 1-bromononane, 1-bromodecane, 1-bromododecane, 1-bromotetradecane, 4-hydroxybenzaldehyde, 4-hydroxybenzoic acid, 4-chlorobenzoic acid, 4-nitrobenzoic acid, terephthalic acid, 1,4-phenylenediamine, 4-nitroaniline, sodium sulphide hydrate, potassium carbonate, potassium iodide, potassium hydroxide, sodium hydroxide, glacial acetic acid, thionyl chloride, methanol, ethanol, acetone, dichloromethane, tetrahydrofuran, *N,N*-dimethylformamide, *n*-hexane, ethyl acetate, and triethylamine. All the chemicals and solvents were used as received without further purification and purchased from Merck, Qrèc (Asia), Sigma-Aldrich, Acros Organics, Fluka, and BDH (British Drug Houses).

3.2. Syntheses

Synthesis of hexakis(4-formlyphenoxy)cyclotriphosphazene, **1.** Intermediate **1** was synthesized according to the method reported by Rong *et al.* (2015) with some modifications.²⁴ 4-Hydroxybenzaldehyde (9.77 g, 0.08 mol) and triethylamine (10.12 g, 0.1 mol) were dissolved in 150 mL acetone and the mixture was cooled to 0 °C in an ice bath. The mixture was stirred for 30 minutes. Then, a solution of hexachlorocyclotriphosphazene (3.48 g, 0.01 mol) in 50 mL acetone was added dropwise to the mixture. A white salt began to precipitate within few minutes. After 2 hours at 0 °C, the reaction was allowed to attain at room temperature and was continued to stir for an additional 94 hours. The reaction was monitored using TLC. Upon completion, the mixture was poured into 250 mL of cold water and left overnight in the fridge. The precipitate formed was then filtered, washed with water and dried. The precipitate was recrystallised from methanol. Yield: 8.11 g (94.19%), mp: 200.8–204.2 °C, white powder. FTIR (cm^{−1}): 2730 (H–C]O), 1699 (C=O stretching), 1595 (C=C stretching), 1205 (C–O stretching), 1151 (P=N stretching), 944 (P–O–C stretching). ¹H-NMR (500 MHz, DMSO-d₆) δ, ppm: 9.90 (s, 1H), 7.78 (d, *J* = 10.0 Hz, 2H), 7.16 (d, *J* = 10.0 Hz, 2H). ¹³C-NMR (125 MHz, DMSO-d₆) δ, ppm: 191.69, 153.59, 133.55, 131.46, 121.03. ³¹P-NMR (500 MHz, DMSO-d₆) δ, ppm: 7.60 (s, 1P). CHN elemental analysis: calculated for C₄₂H₃₀N₃O₁₂P₃: C: 58.55%, H: 3.51%, N: 4.88%; found: C: 58.28%, H: 3.48%, N: 4.83%.

Synthesis of 4-(alkoxy)benzoic acid, **2a–e**

4-(Heptyloxy)benzoic acid, **2a.** Intermediate **2a** was synthesized according to the method reported by Chun-Chieh *et al.* (2016) with some modifications.⁴³ Methyl-4-hydroxybenzoate (15.20 g, 0.10 mol) and 1-bromoheptane (17.89 g, 0.10 mol) dissolved in 20 mL DMF separately, were mixed in a 100 mL round bottom flask. Potassium carbonate (20.73 g, 0.15 mol) and potassium iodide (1.66 g, 0.01 mol) were added to the mixture and was refluxed for 12 hours. Upon completion, the mixture was poured into 300 mL cold water and the precipitate formed was filtered. The precipitate was mixed with potassium hydroxide, KOH (11.22 g, 0.20 mol) in 150 mL ethanol. The mixture was refluxed for 3 hours. All the reaction progress was monitored by TLC. The mixture was then poured into 300 mL water and a clear solution was formed. HCl was added to the solution and the mixture was stirred slowly until the precipitate was formed. The precipitate was filtered, washed with water and dried overnight to obtain a white powder. The same method was used to synthesis **2b–e**. Yield: 20.23 g (85.72%), mp: 105.2–106.5 °C, white powder. FTIR (cm^{−1}): 3250 (O–H stretching), 2919 and 2850 (Csp³–H stretching), 1684 (C=O stretching), 1607 (aromatic C=C stretching), 1252 (C–O stretching). ¹H-NMR (500 MHz, CDCl₃) δ, ppm: 7.78 (d, *J* = 5.0 Hz, 2H), 6.73 (d, *J* = 10.0 Hz, 2H), 3.96 (t, *J* = 7.5 Hz, 2H), 1.68–1.74 (m, 2H), 1.40–1.46 (m, 2H), 1.27–1.38 (m, 6H), 0.89 (t, *J* = 7.5 Hz, 3H). ¹³C-NMR (125 MHz, CDCl₃) δ, ppm: 168.78, 158.91, 135.20, 130.31, 112.80, 67.73, 31.09, 28.83, 28.28, 25.44, 21.82, 13.60. CHN elemental analysis: calculated for C₁₄H₂₀O₃: C: 71.16%, H: 8.53%; found: C: 71.01%, H: 8.57%.



4-(Nonyloxy)benzoic acid, 2b. 1-Bromononane (20.69 g, 0.10 mol) was used in the reaction. Yield: 22.31 g (84.51%), mp: 104.8–105.7 °C, white powder. FTIR (cm^{−1}): 3250 (O–H stretching), 2919 and 2849 (Csp³–H stretching), 1694 (C=O stretching), 1606 (aromatic C=C stretching), 1252 (C–O stretching). ¹H-NMR (500 MHz, CDCl₃) δ, ppm: 7.80 (d, *J* = 10.0 Hz, 2H), 6.74 (d, *J* = 5.0 Hz, 2H), 3.97 (t, *J* = 5.0 Hz, 2H), 1.69–1.74 (m, 2H), 1.41–1.47 (m, 2H), 1.27–1.39 (m, 10H), 0.88 (t, *J* = 5.0 Hz, 3H). ¹³C-NMR (125 MHz, CDCl₃) δ, ppm: 169.36, 159.16, 134.83, 130.37, 113.02, 67.95, 31.10, 28.84, 28.76, 28.62, 28.39, 25.46, 21.80, 13.48. CHN elemental analysis: calculated for C₁₆H₂₄O₃: C: 72.69%, H: 9.15%; found: C: 71.95%, H: 9.15%.

4-(Decyloxy)benzoic acid, 2c. 1-Bromodecane (22.09 g, 0.10 mol) was used in the reaction. Yield: 23.68 g (85.18%), mp: 104.1–105.3 °C, white powder. FTIR (cm^{−1}): 3253 (O–H stretching), 2920 and 2849 (Csp³–H stretching), 1694 (C=O stretching), 1606 (aromatic C=C stretching), 1251 (C–O stretching). ¹H-NMR (500 MHz, CDCl₃) δ, ppm: 7.78 (d, *J* = 10.0 Hz, 2H), 6.73 (d, *J* = 10.0 Hz, 2H), 3.96 (t, *J* = 5.0 Hz, 2H), 1.68–1.73 (m, 2H), 1.40–1.46 (m, 2H), 1.26–1.36 (m, 12H), 0.87 (t, *J* = 7.5 Hz, 3H). ¹³C-NMR (125 MHz, CDCl₃) δ, ppm: 168.78, 159.00, 134.78, 130.36, 112.83, 67.73, 31.13, 28.82, 28.80, 28.77, 28.63, 28.47, 25.45, 21.85, 13.60. CHN elemental analysis: calculated for C₁₇H₂₆O₃: C: 73.35%, H: 9.41%; found: C: 73.14%, H: 9.35%.

4-(Dodecyloxy)benzoic acid, 2d. 1-Bromododecane (24.89 g, 0.10 mol) was used in the reaction. Yield: 26.88 g (87.84%), mp: 104.2–105.6 °C, white powder. FTIR (cm^{−1}): 3250 (O–H stretching), 2920 and 2850 (Csp³–H stretching), 1702 (C=O stretching), 1603 (aromatic C=C stretching), 1250 (C–O stretching). ¹H-NMR (500 MHz, CDCl₃) δ, ppm: 7.83 (d, *J* = 5.0 Hz, 2H), 6.84 (d, *J* = 10.0 Hz, 2H), 4.00 (t, *J* = 7.5 Hz, 2H), 1.69–1.75 (m, 2H), 1.40–1.44 (m, 2H), 1.26–1.35 (m, 16H), 0.87 (t, *J* = 5.0 Hz, 3H). ¹³C-NMR (125 MHz, CDCl₃) δ, ppm: 167.95, 160.55, 134.78, 130.75, 113.53, 67.88, 31.13, 28.83, 28.81, 28.79, 28.78, 28.67, 28.58, 28.47, 25.39, 21.85, 13.59. CHN elemental analysis: calculated for C₁₉H₃₀O₃: C: 74.47%, H: 9.87%; found: C: 73.74%, H: 9.98%.

4-Tetradecyloxybenzoic acid, 2e. 1-Bromotetradecane (27.73 g, 0.10 mol) was used in the reaction. Yield: 28.12 g (84.19%), mp: 103.8–104.7 °C, white powder. FTIR (cm^{−1}): 3251 (O–H stretching), 2919 and 2850 (Csp³–H stretching), 1701 (C=O stretching), 1607 (aromatic C=C stretching), 1252 (C–O stretching). ¹H-NMR (500 MHz, CDCl₃) δ, ppm: 7.80 (d, *J* = 5.0 Hz, 2H), 6.74 (d, *J* = 10.0 Hz, 2H), 3.97 (t, *J* = 5.0 Hz, 2H), 1.68–1.74 (m, 2H), 1.40–1.46 (m, 2H), 1.20–1.36 (m, 20H), 0.87 (t, *J* = 7.5 Hz, 3H). ¹³C-NMR (125 MHz, CDCl₃) δ, ppm: 169.18, 159.27, 134.27, 130.42, 113.02, 67.91, 31.11, 28.83, 28.82, 28.81, 28.80, 28.79, 28.77, 28.76, 28.59, 28.44, 25.44, 21.80, 13.49. CHN elemental analysis: calculated for C₂₁H₃₄O₃: C: 75.41%, H: 10.25%; found: C: 74.51%, H: 10.15%.

Synthesis of 4-(substituted)-N-(4-nitrophenyl)benzamide, 3a–h

4-(Heptyloxy)-N-(4-nitrophenyl)benzamide, 3a. Intermediate 3a was synthesized according to the method reported by Davidson *et al.* (2006) with some modifications.⁴⁴ 4-Heptyloxybenzoic

acid, 2a (7.08 g, 0.03 mol) and thionyl chloride (3.57 g, 0.03 mol) in 40 mL DCM was mixed in 100 mL round bottom flask to form an acid chloride. The mixture was stirred at room temperature for 2 hours to form a clear solution. A solution of 4-nitroaniline (4.14 g, 0.03 mol) in 20 mL THF was added dropwise to the mixture and a white precipitate began to form. Triethylamine, Et₃N (1.52 g, 0.015 mol) was finally added and the mixture was stirred for 8 hours. All the reactions progress are monitored by TLC. The precipitate formed was filtered and the filtrate was collected. After it was dried, the product formed was recrystallised from methanol. The same method was used to synthesis 3b–h. Yield: 7.56 g (70.79%), mp: 137.1–139.8 °C, yellow powder. FTIR (cm^{−1}): 3357 (N–H stretching), 2932 and 2854 (Csp³–H stretching), 1660 (C=O stretching), 1598 (aromatic C=C stretching), 1248 (C–O stretching), 1176 (C–N stretching). ¹H-NMR (500 MHz, CDCl₃) δ, ppm: 10.61 (s, 1H), 8.23 (d, *J* = 5.0 Hz, 2H), 8.03 (d, *J* = 5.0 Hz, 2H), 7.95 (d, *J* = 10.0 Hz, 2H), 7.04 (d, *J* = 10.0 Hz, 2H), 4.03 (t, *J* = 7.5 Hz, 2H), 1.68–1.74 (m, 2H), 1.36–1.42 (m, 2H), 1.23–1.33 (m, 6H), 0.85 (t, *J* = 7.5 Hz, 3H). ¹³C-NMR (125 MHz, CDCl₃) δ, ppm: 166.15, 162.59, 146.09, 143.42, 130.26, 126.95, 124.78, 120.56, 115.03, 68.82, 31.51, 29.08, 28.66, 25.81, 22.22, 13.94. CHN elemental analysis: calculated for C₂₀H₂₄N₂O₄: C: 67.40%, H: 6.79%, N: 7.86%; found: C: 66.81%, H: 6.84%, N: 7.77%.

4-(Nonyloxy)-N-(4-nitrophenyl)benzamide, 3b. Intermediate 2b (7.92 g, 0.03 mol) was used in the reaction. Yield: 7.90 g (68.58%), mp: 136.3–138.2 °C, yellow powder. FTIR (cm^{−1}): 3349 (N–H stretching), 2921 and 2851 (Csp³–H stretching), 1660 (C=O stretching), 1601 (aromatic C=C stretching), 1248 (C–O stretching), 1176 (C–N stretching). ¹H-NMR (500 MHz, CDCl₃) δ, ppm: 10.22 (s, 1H), 8.18 (d, *J* = 10.0 Hz, 2H), 8.00 (d, *J* = 10.0 Hz, 2H), 7.96 (d, *J* = 10.0 Hz, 2H), 7.03 (d, *J* = 10.0 Hz, 2H), 4.09 (t, *J* = 5.0 Hz, 2H), 1.73–1.78 (m, 2H), 1.42–1.48 (m, 2H), 1.25–1.39 (m, 10H), 0.87 (t, *J* = 7.5 Hz, 3H). ¹³C-NMR (125 MHz, CDCl₃) δ, ppm: 166.26, 162.50, 145.95, 143.26, 130.27, 126.65, 124.87, 120.56, 114.93, 68.66, 31.54, 29.17, 29.00, 28.95, 28.83, 25.77, 22.29, 14.04. CHN elemental analysis: calculated for C₂₂H₂₈N₂O₄: C: 68.73%, H: 7.34%, N: 7.29%; found: C: 68.03%, H: 7.39%, N: 7.27%.

4-(Decyloxy)-N-(4-nitrophenyl)benzamide, 3c. Intermediate 2c (8.24 g, 0.03 mol) was used in the reaction. Yield: 8.66 g (72.53%), mp: 135.5–137.1 °C, yellow powder. FTIR (cm^{−1}): 3346 (N–H stretching), 2919 and 2851 (Csp³–H stretching), 1657 (C=O stretching), 1598 (aromatic C=C stretching), 1246 (C–O stretching), 1176 (C–N stretching). ¹H-NMR (500 MHz, CDCl₃) δ, ppm: 10.33 (s, 1H), 8.19 (d, *J* = 10.0 Hz, 2H), 8.00 (d, *J* = 5.0 Hz, 2H), 7.95 (d, *J* = 5.0 Hz, 2H), 7.03 (d, *J* = 10.0 Hz, 2H), 4.07 (t, *J* = 7.5 Hz, 2H), 1.70–1.76 (m, 2H), 1.39–1.45 (m, 2H), 1.22–1.36 (m, 12H), 0.85 (t, *J* = 7.5 Hz, 3H). ¹³C-NMR (125 MHz, CDCl₃) δ, ppm: 166.18, 162.51, 146.05, 143.24, 130.29, 126.72, 124.89, 120.52, 114.93, 68.66, 31.59, 29.24, 29.20, 29.02, 28.99, 28.92, 25.80, 22.32, 14.07. CHN elemental analysis: calculated for C₂₃H₃₀N₂O₄: C: 69.32%, H: 7.59%, N: 7.03%; found: C: 69.12%, H: 7.59%, N: 6.99%.

4-(Dodecyloxy)-N-(4-nitrophenyl)benzamide, 3d. Intermediate 2d (9.18 g, 0.03 mol) was used in the reaction. Yield: 9.15 g (71.60%), mp: 133.4–135.8 °C, yellow powder. FTIR (cm^{−1}): 3344



(N–H stretching), 2916 and 2849 (Csp³–H stretching), 1657 (C=O stretching), 1598 (aromatic C=C stretching), 1248 (C–O stretching), 1176 (C–N stretching). ¹H-NMR (500 MHz, CDCl₃) δ, ppm: 10.25 (s, 1H), 8.16 (d, *J* = 10.0 Hz, 2H), 7.96 (d, *J* = 5.0 Hz, 2H), 7.92 (d, *J* = 10.0 Hz, 2H), 7.00 (d, *J* = 10.0 Hz, 2H), 4.05 (t, *J* = 5.0 Hz, 2H), 1.68–1.74 (m, 2H), 1.37–1.43 (m, 2H), 1.19–1.34 (m, 16H), 0.82 (t, *J* = 5.0 Hz, 3H). ¹³C-NMR (125 MHz, CDCl₃) δ, ppm: 166.31, 162.52, 146.90, 143.32, 130.24, 126.65, 124.86, 120.61, 114.97, 68.69, 31.54, 29.23, 29.22, 29.18, 29.16, 29.15, 28.93, 28.88, 25.74, 22.27, 13.99. CHN elemental analysis: calculated for C₂₅H₃₄N₂O₄: C: 70.40%, H: 8.03%, N: 6.57%; found: C: 70.06%, H: 8.03%, N: 6.50%.

4-(Tetradecyloxy)-N-(4-nitrophenyl)benzamide, 3e. Intermediate 2e (10.02 g, 0.03 mol) was used in the reaction. Yield: 9.68 g (71.07%), mp: 131.7–133.6 °C, yellow powder. FTIR (cm⁻¹): 3343 (N–H stretching), 2916 and 2851 (Csp³–H stretching), 1657 (C=O stretching), 1606 (aromatic C=C stretching), 1254 (C–O stretching), 1178 (C–N stretching). ¹H-NMR (500 MHz, CDCl₃) δ, ppm: 10.25 (s, 1H), 8.17 (d, *J* = 5.0 Hz, 2H), 7.96 (d, *J* = 5.0 Hz, 2H), 7.92 (d, *J* = 10.0 Hz, 2H), 7.01 (d, *J* = 5.0 Hz, 2H), 4.05 (t, *J* = 5.0 Hz, 2H), 1.69–1.74 (m, 2H), 1.37–1.43 (m, 2H), 1.17–1.36 (m, 20H), 0.82 (t, *J* = 5.0 Hz, 3H). ¹³C-NMR (125 MHz, CDCl₃) δ, ppm: 166.32, 162.53, 146.91, 143.33, 130.25, 126.66, 124.86, 120.61, 114.98, 68.70, 31.55, 29.25, 29.23, 29.22, 29.19, 29.18, 29.16, 29.15, 28.94, 28.89, 25.75, 22.28, 14.00. CHN elemental analysis: calculated for C₂₇H₃₈N₂O₄: C: 71.34%, H: 8.43%, N: 6.16%; found: C: 70.68%, H: 8.38%, N: 6.12%.

4-(Hydroxy)-N-(4-nitrophenyl)benzamide, 3f. 4-Hydroxybenzoic acid (4.14 g, 0.03 mol) was used in the reaction. Yield: 5.66 g (73.13%), mp: 163.6–165.2 °C, yellow powder. FTIR (cm⁻¹): 3340 (N–H stretching), 3201 (O–H stretching), 1698 (C=O stretching), 1600 (aromatic C=C stretching), 1252 (C–O stretching), 1175 (C–N stretching). ¹H-NMR (500 MHz, CDCl₃) δ, ppm: 9.72 (s, 1H), 8.04 (d, *J* = 5.0 Hz, 2H), 7.71 (d, *J* = 10.0 Hz, 2H), 6.90 (d, *J* = 5.0 Hz, 2H), 6.88 (d, *J* = 10.0 Hz, 2H). ¹³C-NMR (125 MHz, CDCl₃) δ, ppm: 166.77, 162.55, 146.89, 143.12, 130.75, 125.80, 124.47, 120.50, 113.96. CHN elemental analysis: calculated for C₁₃H₁₀N₂O₄: C: 60.47%, H: 3.90%, N: 10.85%; found: C: 60.10%, H: 3.88%, N: 10.79%.

4-(Carboxy)-N-(4-nitrophenyl)benzamide, 3g. Terephthalic acid (4.98 g, 0.03 mol) was used in the reaction. Yield: 5.12 g (59.67%), mp: 168.7–170.8 °C, light brown powder. FTIR (cm⁻¹): 3341 (N–H stretching), 3100–3270 (O–H stretching), 1700 (C=O stretching), 1606 (aromatic C=C stretching), 1248 (C–O stretching), 1177 (C–N stretching). ¹H-NMR (500 MHz, CDCl₃) δ, ppm: 11.06 (s, 1H), 10.07 (s, 1H), 8.10 (d, *J* = 10.0 Hz, 2H), 8.08 (d, *J* = 5.0 Hz, 2H), 7.98 (d, *J* = 10.0 Hz, 2H), 6.90 (d, *J* = 10.0 Hz, 2H). ¹³C-NMR (125 MHz, CDCl₃) δ, ppm: 167.03, 164.33, 140.06, 139.29, 136.08, 130.55, 130.34, 129.94, 126.57, 116.19. CHN elemental analysis: calculated for C₁₄H₁₀N₂O₅: C: 58.75%, H: 3.52%, N: 9.79%; found: C: 58.43%, H: 3.50%, N: 9.80%.

4-(Chloro)-N-(4-nitrophenyl)benzamide, 3h. 4-Chlorobenzoic acid (4.69 g, 0.03 mol) was used in the reaction. Yield: 6.11 g (73.67%), mp: 155.1–157.4 °C, yellow powder. FTIR (cm⁻¹): 3342 (N–H stretching), 1691 (C=O stretching), 1602 (aromatic C=C stretching), 1250 (C–O stretching), 1170 (C–N stretching), 827 (C–Cl bending). ¹H-NMR (500 MHz, CDCl₃) δ, ppm: 9.90 (s, 1H),

8.02 (d, *J* = 10.0 Hz, 2H), 7.83 (d, *J* = 10.0 Hz, 2H), 7.55 (d, *J* = 5.0 Hz, 2H), 6.87 (d, *J* = 5.0 Hz, 2H). ¹³C-NMR (125 MHz, CDCl₃) δ, ppm: 166.58, 162.51, 146.91, 143.21, 130.69, 125.84, 124.57, 121.22, 117.10. CHN elemental analysis: calculated for C₁₃H₉ClN₂O₃: C: 56.44%, H: 3.28%, N: 12.81%; found: C: 56.27%, H: 3.25%, N: 12.76%.

Reduction of intermediates 3a–h to afford 4a–h

N-(4-Aminophenyl)-4-(heptyloxy)benzamide, 4a. Intermediate 4a was synthesized according to the method reported by Shaoyu and Jiangbing (2012) with some modifications.⁴⁵ A solution of intermediate 3a (5.00 g, 0.014 mmol) in 40 mL ethanol and a solution of sodium sulphide hydrate, Na₂S·9H₂O (0.89 g, 0.01 mol) in 20 mL ethanol and 20 mL water were mixed in 250 mL round bottom flask. The mixture was refluxed for 12 hours. The reaction progress was monitored by TLC. Upon completion, the mixture was cooled in an ice bath. The precipitate formed was filtered, washed with cold ethanol and dried to form a white precipitate. The same method was used to synthesis 4b–h. Yield: 3.55 g (77.53%), mp: 155.3–157.1 °C, white powder. FTIR (cm⁻¹): 3330 (N–H amide stretching), 3403 and 3204 (N–H amine stretching), 2921 and 2854 (Csp³–H stretching), 1696 (C=O stretching), 1609 (aromatic C=C stretching), 1254 (C–O stretching), 1173 (C–N stretching). ¹H-NMR (500 MHz, CDCl₃) δ, ppm: 9.69 (s, 1H), 7.89 (d, *J* = 5.0 Hz, 2H), 7.34 (d, *J* = 5.0 Hz, 2H), 7.00 (d, *J* = 5.0 Hz, 2H), 6.53 (d, *J* = 10.0 Hz, 2H), 4.87 (s, 2H), 4.02 (t, *J* = 5.0 Hz, 2H), 1.69–1.75 (m, 2H), 1.38–1.44 (m, 2H), 1.25–1.36 (m, 6H), 0.86 (t, *J* = 7.5 Hz, 3H). ¹³C-NMR (125 MHz, CDCl₃) δ, ppm: 164.64, 161.46, 145.46, 129.72, 128.76, 127.64, 122.74, 114.38, 114.17, 68.15, 31.68, 29.05, 28.87, 25.90, 22.50, 14.40. CHN elemental analysis: calculated for C₂₀H₂₆N₂O₂: C: 73.59%, H: 8.03%, N: 8.58%; found: C: 73.26%, H: 8.08%, N: 8.51%.

N-(4-Aminophenyl)-4-(nonyloxy)benzamide, 4b. Intermediate 3b (5.00 g, 0.013 mol) was used in the reaction. Yield: 3.60 g (78.09%), mp: 153.7–154.9 °C, white powder. FTIR (cm⁻¹): 3340 (N–H amide stretching), 3410 and 3201 (N–H amine stretching), 2919 and 2851 (Csp³–H stretching), 1698 (C=O stretching), 1609 (aromatic C=C stretching), 1254 (C–O stretching), 1178 (C–N stretching). ¹H-NMR (500 MHz, CDCl₃) δ, ppm: 9.69 (s, 1H), 7.88 (d, *J* = 10.0 Hz, 2H), 7.33 (d, *J* = 10.0 Hz, 2H), 6.99 (d, *J* = 10.0 Hz, 2H), 6.53 (d, *J* = 10.0 Hz, 2H), 4.87 (s, 2H), 4.02 (t, *J* = 5.0 Hz, 2H), 1.69–1.74 (m, 2H), 1.38–1.43 (m, 2H), 1.22–1.35 (m, 10H), 0.85 (t, *J* = 5.0 Hz, 3H). ¹³C-NMR (125 MHz, CDCl₃) δ, ppm: 164.64, 161.46, 145.46, 129.72, 128.75, 127.63, 122.75, 114.38, 114.18, 68.15, 31.72, 29.40, 29.21, 29.09, 29.04, 25.92, 22.55, 14.41. CHN elemental analysis: calculated for C₂₂H₃₀N₂O₂: C: 74.54%, H: 8.53%, N: 7.90%; found: C: 74.31%, H: 8.54%, N: 7.88%.

N-(4-Aminophenyl)-4-(decyloxy)benzamide, 4c. Intermediate 3c (5.00 g, 0.013 mol) was used in the reaction. Yield: 3.58 g (77.44%), mp: 153.4–154.1 °C, white powder. FTIR (cm⁻¹): 3340 (N–H amide stretching), 3404 and 3213 (N–H amine stretching), 2919 and 2851 (Csp³–H stretching), 1700 (C=O stretching), 1606 (aromatic C=C stretching), 1254 (C–O stretching), 1176 (C–N stretching). ¹H-NMR (500 MHz, CDCl₃) δ, ppm: 9.68 (s, 1H), 7.89 (d, *J* = 10.0 Hz, 2H), 7.34 (d, *J* = 10.0 Hz, 2H), 7.00 (d, *J* = 10.0 Hz, 2H), 6.53 (d, *J* = 10.0 Hz, 2H), 4.87 (s, 2H), 4.03 (t, *J* =



7.5 Hz, 2H), 1.69–1.75 (m, 2H), 1.38–1.44 (m, 2H), 1.22–1.35 (m, 12H), 0.86 (t, J = 7.5 Hz, 3H). ^{13}C -NMR (125 MHz, CDCl_3) δ , ppm: 164.57, 161.45, 145.48, 129.72, 128.77, 127.69, 122.73, 114.38, 114.15, 68.15, 31.75, 29.45, 29.40, 29.21, 29.15, 29.05, 25.93, 22.55, 14.42. CHN elemental analysis: calculated for $\text{C}_{23}\text{H}_{32}\text{N}_2\text{O}_2$: C: 74.96%, H: 8.75%, N: 7.60%; found: C: 74.65%, H: 8.75%, N: 7.57%.

N-(4-Aminophenyl)-4-(dodecyloxy)benzamide, 4d. Intermediate **3d** (5.00 g, 0.012 mol) was used in the reaction. Yield: 3.61 g (78.32%), mp: 151.8–153.4 °C, yellow powder. FTIR (cm⁻¹): 3352 (N–H amide stretching), 3402 and 3206 (N–H amine stretching), 2919 and 2851 (Csp^3 –H stretching), 1698 (C=O stretching), 1606 (aromatic C=C stretching), 1254 (C–O stretching), 1178 (C–N stretching). ^1H -NMR (500 MHz, CDCl_3) δ , ppm: 9.69 (s, 1H), 7.89 (d, J = 10.0 Hz, 2H), 7.34 (d, J = 10.0 Hz, 2H), 7.00 (d, J = 5.0 Hz, 2H), 6.53 (d, J = 10.0 Hz, 2H), 4.87 (s, 2H), 4.02 (t, J = 7.5 Hz, 2H), 1.69–1.75 (m, 2H), 1.38–1.44 (m, 2H), 1.22–1.34 (m, 16H), 0.85 (t, J = 5.0 Hz, 3H). ^{13}C -NMR (125 MHz, CDCl_3) δ , ppm: 164.62, 161.45, 145.47, 129.72, 128.77, 127.65, 122.74, 114.37, 114.16, 68.14, 31.75, 29.48, 29.46, 29.44, 29.43, 29.19, 29.16, 29.04, 25.92, 22.55, 14.41. CHN elemental analysis: calculated for $\text{C}_{25}\text{H}_{36}\text{N}_2\text{O}_2$: C: 75.72%, H: 9.15%, N: 7.06%; found: C: 75.56%, H: 9.13%, N: 7.01%.

N-(4-Aminophenyl)-4-(tetradecyloxy)benzamide, 4e. Intermediate **3e** (5.00 g, 0.011 mol) was used in the reaction. Yield: 3.66 g (78.38%), mp: 150.6–152.8 °C, yellow powder. FTIR (cm⁻¹): 3345 (N–H amide stretching), 3411 and 3203 (N–H amine stretching), 2921 and 2851 (Csp^3 –H stretching), 1698 (C=O stretching), 1606 (aromatic C=C stretching), 1256 (C–O stretching), 1176 (C–N stretching). ^1H -NMR (500 MHz, CDCl_3) δ , ppm: 9.31 (s, 1H), 7.88 (d, J = 10.0 Hz, 2H), 7.34 (d, J = 10.0 Hz, 2H), 6.98 (d, J = 5.0 Hz, 2H), 6.59 (d, J = 5.0 Hz, 2H), 4.06 (t, J = 7.5 Hz, 2H), 1.73–1.77 (m, 2H), 1.41–1.46 (m, 2H), 1.25–1.38 (m, 20H), 0.87 (t, J = 7.5 Hz, 3H). ^{13}C -NMR (125 MHz, CDCl_3) δ , ppm: 164.94, 161.69, 145.25, 131.67, 129.63, 129.39, 122.94, 114.74, 114.60, 68.65, 31.62, 29.34, 29.33, 29.31, 29.27, 29.26, 29.24, 29.12, 29.06, 28.96, 25.86, 22.31, 14.02. CHN elemental analysis: calculated for $\text{C}_{27}\text{H}_{40}\text{N}_2\text{O}_2$: C: 76.37%, H: 9.50%, N: 6.60%; found: C: 76.18%, H: 9.47%, N: 6.62%.

N-(4-Aminophenyl)-4-(hydroxy)benzamide, 4f. Intermediate **3f** (5.00 g, 0.019 mol) was used in the reaction. Yield: 3.22 g (72.87%), mp: 211.1–213.6 °C, white powder. FTIR (cm⁻¹): 3340 (N–H amide stretching), 3405 and 3211 (N–H amine stretching), 3200 (O–H stretching), 1691 (C=O stretching), 1609 (aromatic C=C stretching), 1254 (C–O stretching), 1178 (C–N stretching). ^1H -NMR (500 MHz, CDCl_3) δ , ppm: 9.73 (s, 1H), 8.24 (d, J = 5.0 Hz, 2H), 8.10 (d, J = 10.0 Hz, 2H), 7.71 (d, J = 10.0 Hz, 2H), 6.89 (d, J = 10.0 Hz, 2H). ^{13}C -NMR (125 MHz, CDCl_3) δ , ppm: 166.28, 163.72, 150.37, 136.75, 132.54, 131.07, 128.83, 124.02, 116.26. CHN elemental analysis: calculated for $\text{C}_{13}\text{H}_{12}\text{N}_2\text{O}_2$: C: 68.41%, H: 5.30%, N: 12.27%; found: C: 68.17%, H: 5.27%, N: 12.19%.

N-(4-Aminophenyl)-4-(carboxy)benzamide, 4g. Intermediate **3g** (4.50 g, 0.016 mol) was used in the reaction. Yield: 3.10 g (76.96%), mp: 232.6–233.9 °C, white powder. FTIR (cm⁻¹): 3351 (N–H amide stretching), 3401 and 3202 (N–H amine stretching), 3203 (O–H stretching), 1692 (C=O stretching), 1608 (aromatic

C=C stretching), 1254 (C–O stretching), 1178 (C–N stretching). ^1H -NMR (500 MHz, CDCl_3) δ , ppm: 10.06 (s, 1H), 8.10 (d, J = 10.0 Hz, 2H), 7.98 (d, J = 5.0 Hz, 2H), 7.92 (d, J = 10.0 Hz, 2H), 6.67 (s, 2H), 6.60 (d, J = 10.0 Hz, 2H). ^{13}C -NMR (125 MHz, CDCl_3) δ , ppm: 167.07, 156.08, 139.27, 136.17, 136.11, 130.34, 129.94, 126.81, 112.86. CHN elemental analysis: calculated for $\text{C}_{14}\text{H}_{12}\text{N}_2\text{O}_3$: C: 65.62%, H: 4.72%, N: 10.93%; found: C: 65.28%, H: 4.70%, N: 10.85%.

N-(4-Aminophenyl)-4-(chloro)benzamide, 4h. Intermediate **3h** (5.00 g, 0.018 mol) was used in the reaction. Yield: 3.05 g (68.43%), mp: 170.4–172.1 °C, white powder. FTIR (cm⁻¹): 3344 (N–H amide stretching), 3473 and 3207 (N–H amine stretching), 1641 (C=O stretching), 1701 (aromatic C=C stretching), 1252 (C–O stretching), 1189 (C–N stretching), 825 (C–Cl bending). ^1H -NMR (500 MHz, CDCl_3) δ , ppm: 10.08 (s, 1H), 8.33 (d, J = 5.0 Hz, 2H), 8.09 (d, J = 10.0 Hz, 2H), 7.88 (d, J = 10.0 Hz, 2H), 6.61 (s, 2H), 6.58 (d, J = 10.0 Hz, 2H). ^{13}C -NMR (125 MHz, CDCl_3) δ , ppm: 166.87, 163.80, 150.45, 136.76, 132.60, 131.29, 128.90, 124.33, 118.11. CHN elemental analysis: calculated for $\text{C}_{13}\text{H}_{11}\text{ClN}_2\text{O}$: C: 63.29%, H: 4.49%, N: 14.37%; found: C: 63.12%, H: 4.50%, N: 14.26%.

Synthesis of *N-(4-aminophenyl)-4-(nitro)benzamide, 4i.* Intermediate **4i** was synthesized according to the method reported by Avdeenko and Marchenko (2001) with some modifications.⁴⁶ A mixture of 4-nitrobenzoic acid (6.21 g, 0.03 mol) and thionyl chloride (3.57 g, 0.03 mol) was dissolved in 20 mL DCM in a 100 mL round bottom flask. The mixture was stirred at room temperature for 2 hours. Upon completion, the corresponding acid chloride which was not isolated was reacted with 1,4-phenylenediamine (6.48 g, 0.06 mol) in 10 mL THF. Then, triethylamine (1.52 g, 0.015 mol) was added dropwise to the mixture and it was left to stir at room temperature for 8 hours. The reaction progress was monitored by TLC. The precipitate formed was filtered and the filtrate was collected. The filtrate was evaporated, dried and purified using column chromatography. Yield: 4.23 g (54.86%), mp: 187.7–189.3 °C, yellow powder. FTIR (cm⁻¹): 3341 (N–H amide stretching), 3408 and 3207 (N–H amine stretching), 1690 (C=O stretching), 1595 (aromatic C=C stretching), 1248 (C–O stretching), 1146 (C–N stretching). ^1H -NMR (500 MHz, CDCl_3) δ , ppm: 9.93 (s, 1H), 7.90 (d, J = 10.0 Hz, 2H), 7.87 (d, J = 5.0 Hz, 2H), 7.59 (d, J = 6.0 Hz, 2H), 6.63 (s, 2H), 6.59 (d, J = 10.0 Hz, 2H). ^{13}C -NMR (125 MHz, CDCl_3) δ , ppm: 166.59, 162.98, 150.10, 136.44, 132.37, 131.10, 128.51, 123.89, 114.70. CHN elemental analysis: calculated for $\text{C}_{14}\text{H}_{12}\text{N}_2\text{O}_3$: C: 65.62%, H: 4.72%, N: 10.93%; found: C: 65.34%, H: 4.69%, N: 10.82%.

Synthesis of hexakis{[(4-(substituted)benzamide)methaneylidene]azaneylylidene}triazaphosphazene, 5a–i

Hexakis{[(4-(heptyloxy)benzamide)methaneylidene]azaneylylidene}triazaphosphazene, 5a. Compound **5a** was synthesized according to the method reported by Jamain *et al.* (2019) and Fareed *et al.* (2013) with some modifications.^{32,47} A mixture of intermediate **1** (0.70 g, 0.81 mmol) and intermediate **4a** (1.86 g, 5.69 mmol) in 50 mL methanol was mixed in a 100 mL round bottom flask. A few drops of glacial acetic acid were added to the solution. The mixture was refluxed for 18 hours. The reaction progress was monitored by TLC. Upon completion, the



precipitate formed was filtered and dried overnight. The product was recrystallised from ethanol. The same method was used to synthesis **5b–h**. Yield: 1.47 g (66.74%), mp: 183.6–185.1 °C, yellow powder. FTIR (cm^{−1}): 3365 (N–H stretching), 2921 and 2854 (Csp³–H stretching), 1691 (C=O stretching), 1644 (C=N stretching), 1592 (aromatic C=C stretching), 1254 (C–O stretching), 1197 (P=N stretching), 1178 (C–N stretching), 977 (P–O–C stretching). ¹H-NMR (500 MHz, DMSO-d₆) δ, ppm: 9.83 (s, 1H), 8.65 (s, 1H), 7.95 (d, *J* = 5.0 Hz, 2H), 7.94 (d, *J* = 5.0 Hz, 2H), 7.80 (d, *J* = 10.0 Hz, 2H), 7.55 (d, *J* = 5.0 Hz, 2H), 7.29 (d, *J* = 10.0 Hz, 2H), 7.02 (d, *J* = 10.0 Hz, 2H), 4.08 (t, *J* = 5.0 Hz, 2H), 1.73–1.79 (m, 2H), 1.42–1.48 (m, 2H), 1.28–1.40 (m, 6H), 0.89 (t, *J* = 5.0 Hz, 3H). ¹³C-NMR (125 MHz, DMSO-d₆) δ, ppm: 165.46, 162.05, 158.11, 146.97, 138.44, 136.35, 135.82, 130.48, 129.94, 129.29, 127.70, 121.74, 121.69, 114.82, 68.65, 31.56, 29.11, 28.71, 25.85, 22.29, 14.06. ³¹P-NMR (500 MHz, DMSO-d₆) δ, ppm: 8.49 (s, 1P). CHN elemental analysis: calculated for C₁₆₂H₁₇₄N₁₅O₁₈P₃: C: 71.74%, H: 6.47%, N: 7.75%; found: C: 71.57%, H: 6.40%, N: 7.71%.

Hexakis{[(4-(nonyloxy)benzamide)methaneyllidene]azaneylylidene}triazaphosphazene, 5b. Intermediate **4b** (2.02 g, 5.69 mmol) was used in the reaction. Yield: 1.53 g (65.41%), mp: 178.1–180.5 °C, yellow powder. FTIR (cm^{−1}): 3365 (N–H stretching), 2919 and 2849 (Csp³–H stretching), 1691 (C=O stretching), 1646 (C=N stretching), 1593 (aromatic C=C stretching), 1256 (C–O stretching), 1197 (P=N stretching), 1178 (C–N stretching), 974 (P–O–C stretching). ¹H-NMR (500 MHz, DMSO-d₆) δ, ppm: 9.82 (s, 1H), 8.65 (s, 1H), 7.96 (d, *J* = 10.0 Hz, 2H), 7.94 (d, *J* = 10.0 Hz, 2H), 7.81 (d, *J* = 10.0 Hz, 2H), 7.54 (d, *J* = 10.0 Hz, 2H), 7.29 (d, *J* = 10.0 Hz, 2H), 7.02 (d, *J* = 10.0 Hz, 2H), 4.08 (t, *J* = 7.5 Hz, 2H), 1.73–1.79 (m, 2H), 1.42–1.48 (m, 2H), 1.24–1.39 (m, 10H), 0.88 (t, *J* = 5.0 Hz, 3H). ¹³C-NMR (125 MHz, DMSO-d₆) δ, ppm: 165.44, 162.05, 158.04, 146.95, 138.46, 136.36, 135.82, 130.46, 129.94, 129.27, 127.71, 121.74, 121.69, 114.80, 68.64, 31.63, 29.28, 29.11, 28.93, 25.89, 22.36, 14.08. ³¹P-NMR (500 MHz, DMSO-d₆) δ, ppm: 8.51 (s, 1P). CHN elemental analysis: calculated for C₁₇₄H₁₉₈N₁₅O₁₈P₃: C: 72.55%, H: 6.93%, N: 7.29%; found: C: 72.04%, H: 6.88%, N: 7.22%.

Hexakis{[(4-decyloxy)benzamide)methaneyllidene]azaneylylidene}triazaphosphazene, 5c. Intermediate **4c** (2.09 g, 5.69 mmol) was used in the reaction. Yield: 1.55 g (64.39%), mp: 175.7–177.6 °C, yellow powder. FTIR (cm^{−1}): 3363 (N–H stretching), 2919 and 2851 (Csp³–H stretching), 1690 (C=O stretching), 1644 (C=N stretching), 1593 (aromatic C=C stretching), 1259 (C–O stretching), 1197 (P=N stretching), 1181 (C–N stretching), 977 (P–O–C stretching). ¹H-NMR (500 MHz, DMSO-d₆) δ, ppm: 9.82 (s, 1H), 8.65 (s, 1H), 7.96 (d, *J* = 10.0 Hz, 2H), 7.94 (d, *J* = 5.0 Hz, 2H), 7.80 (d, *J* = 10.0 Hz, 2H), 7.55 (d, *J* = 5.0 Hz, 2H), 7.29 (d, *J* = 10.0 Hz, 2H), 7.03 (d, *J* = 5.0 Hz, 2H), 4.08 (t, *J* = 7.5 Hz, 2H), 1.73–1.78 (m, 2H), 1.42–1.48 (m, 2H), 1.24–1.38 (m, 12H), 0.88 (t, *J* = 7.5 Hz, 3H). ¹³C-NMR (125 MHz, DMSO-d₆) δ, ppm: 165.46, 162.05, 158.10, 146.96, 138.43, 136.36, 135.81, 130.47, 129.94, 129.28, 127.69, 121.75, 121.69, 114.81, 68.64, 31.63, 29.30, 29.26, 29.09, 28.97, 25.87, 22.34, 14.07. ³¹P-NMR (500 MHz, DMSO-d₆) δ, ppm: 8.48 (s, 1P). CHN elemental analysis: calculated for C₁₈₀H₂₁₀N₁₅O₁₈P₃: C: 72.92%, H: 7.14%, N: 7.09%; found: C: 72.76%, H: 7.11%, N: 7.02%.

Hexakis{[(4-(dodecyloxy)benzamide)methaneyllidene]azaneylylidene}triazaphosphazene, 5d. Intermediate **4d** (2.25 g, 5.69 mmol) was used in the reaction. Yield: 1.66 g (65.25%), mp: 171.3–173.8 °C, yellow powder. FTIR (cm^{−1}): 3363 (N–H stretching), 2916 and 2851 (Csp³–H stretching), 1695 (C=O stretching), 1644 (C=N stretching), 1592 (aromatic C=C stretching), 1255 (C–O stretching), 1197 (P=N stretching), 1178 (C–N stretching), 978 (P–O–C stretching). ¹H-NMR (500 MHz, DMSO-d₆) δ, ppm: 9.82 (s, 1H), 8.65 (s, 1H), 7.95 (d, *J* = 10.0 Hz, 2H), 7.94 (d, *J* = 5.0 Hz, 2H), 7.80 (d, *J* = 10.0 Hz, 2H), 7.54 (d, *J* = 10.0 Hz, 2H), 7.29 (d, *J* = 10.0 Hz, 2H), 7.02 (d, *J* = 10.0 Hz, 2H), 4.07 (t, *J* = 7.5 Hz, 2H), 1.72–1.78 (m, 2H), 1.42–1.48 (m, 2H), 1.24–1.37 (m, 16H), 0.87 (t, *J* = 7.5 Hz, 3H). ¹³C-NMR (125 MHz, DMSO-d₆) δ, ppm: 165.46, 162.04, 158.07, 146.96, 138.42, 136.36, 135.80, 130.46, 129.93, 129.27, 127.68, 121.75, 121.68, 114.80, 68.63, 31.63, 29.35, 29.32, 29.29, 29.09, 29.08, 28.98, 25.87, 22.34, 14.06. ³¹P-NMR (500 MHz, DMSO-d₆) δ, ppm: 8.50 (s, 1P). CHN elemental analysis: calculated for C₁₉₂H₂₃₄N₁₅O₁₈P₃: C: 73.61%, H: 7.53%, N: 6.71%; found: C: 73.23%, H: 7.48%, N: 6.65%.

Hexakis{[(4-(tetradecyloxy)benzamide)methaneyllidene]azaneylylidene}triazaphosphazene, 5e. Intermediate **4e** (2.41 g, 5.69 mmol) was used in the reaction. Yield: 1.84 g (68.64%), mp: 168.5–170.5 °C, yellow powder. FTIR (cm^{−1}): 3317 (N–H stretching), 2921 and 2849 (Csp³–H stretching), 1691 (C=O stretching), 1641 (C=N stretching), 1599 (aromatic C=C stretching), 1259 (C–O stretching), 1189 (P=N stretching), 1178 (C–N stretching), 977 (P–O–C stretching). ¹H-NMR (500 MHz, DMSO-d₆) δ, ppm: 9.82 (s, 1H), 8.64 (s, 1H), 7.95 (d, *J* = 10.0 Hz, 2H), 7.94 (d, *J* = 5.0 Hz, 2H), 7.81 (d, *J* = 5.0 Hz, 2H), 7.54 (d, *J* = 5.0 Hz, 2H), 7.29 (d, *J* = 10.0 Hz, 2H), 7.02 (d, *J* = 5.0 Hz, 2H), 4.07 (t, *J* = 7.5 Hz, 2H), 1.72–1.78 (m, 2H), 1.42–1.47 (m, 2H), 1.22–1.38 (m, 20H), 0.87 (t, *J* = 7.5 Hz, 3H). ¹³C-NMR (125 MHz, DMSO-d₆) δ, ppm: 165.44, 162.04, 158.04, 146.95, 138.44, 136.36, 135.81, 130.45, 129.93, 129.27, 127.69, 121.74, 121.67, 114.79, 68.63, 31.64, 29.37, 29.36, 29.35, 29.34, 29.29, 29.11, 29.09, 28.97, 25.87, 22.34, 14.05. ³¹P-NMR (500 MHz, DMSO-d₆) δ, ppm: 8.47 (s, 1P). CHN elemental analysis: calculated for C₂₀₄H₂₅₈N₁₅O₁₈P₃: C: 74.22%, H: 7.88%, N: 6.36%; found: C: 73.89%, H: 7.80%, N: 6.31%.

Hexakis{[(4-(hydroxy)benzamide)methaneyllidene]azaneylylidene}triazaphosphazene, 5f. Intermediate **4f** (1.30 g, 5.69 mmol) was used in the reaction. Yield: 1.23 g (71.33%), mp: 282.7–285.1 °C, yellow powder. FTIR (cm^{−1}): 3356 (N–H stretching), 3260 (O–H stretching), 1697 (C=O stretching), 1640 (C=N stretching), 1590 (aromatic C=C stretching), 1253 (C–O stretching), 1190 (P=N stretching), 1152 (C–N stretching), 980 (P–O–C stretching). ¹H-NMR (500 MHz, DMSO-d₆) δ, ppm: 8.42 (s, 1H), 7.94 (d, *J* = 5.0 Hz, 2H), 7.73 (d, *J* = 10.0 Hz, 2H), 7.50 (d, *J* = 10.0 Hz, 2H), 7.12 (d, *J* = 10.0 Hz, 2H), 6.88 (d, *J* = 10.0 Hz, 2H), 6.80 (d, *J* = 10.0 Hz, 2H). ¹³C-NMR (125 MHz, DMSO-d₆) δ, ppm: 167.05, 160.60, 157.36, 156.14, 143.65, 138.25, 131.57, 130.67, 130.23, 129.09, 128.33, 122.59, 116.17, 116.07. ³¹P-NMR (500 MHz, DMSO-d₆) δ, ppm: 8.52 (s, 1P). CHN elemental analysis: calculated for C₁₂₀H₉₀N₁₅O₁₈P₃: C: 67.89%, H: 4.27%, N: 9.90%; found: C: 67.70%, H: 4.23%, N: 9.86%.



Hexakis{[(4-(carboxy)benzamide)methaneylidene]azaneylylidene}triazaphosphazene, 5g. Intermediate **4g** (1.46 g, 5.69 mmol) was used in the reaction. Yield: 1.31 g (70.39%), mp: 296.1–298.5 °C, orange powder. FTIR (cm⁻¹): 3336 (N–H stretching), 3290 (O–H stretching), 1699 (C=O stretching), 1642 (C=N stretching), 1601 (aromatic C=C stretching), 1254 (C–O stretching), 1190 (P=N stretching), 1174 (C–N stretching), 978 (P–O–C stretching). ¹H-NMR (500 MHz, DMSO-d₆) δ, ppm: 8.61 (s, 1H), 8.21 (d, *J* = 10.0 Hz, 2H), 8.10 (d, *J* = 5.0 Hz, 2H), 8.01 (d, *J* = 10.0 Hz, 2H), 7.94 (d, *J* = 5.0 Hz, 2H), 7.22 (d, *J* = 10.0 Hz, 2H), 6.82 (d, *J* = 5.0 Hz, 2H). ¹³C-NMR (125 MHz, DMSO-d₆) δ, ppm: 167.47, 166.28, 157.21, 156.28, 150.29, 142.55, 140.52, 136.92, 131.02, 130.09, 128.60, 123.95, 123.19, 116.24. ³¹P-NMR (500 MHz, DMSO-d₆) δ, ppm: 8.57 (s, 1P). CHN elemental analysis: calculated for C₁₂₆H₉₀N₁₅O₂₄P₃: C: 66.05%, H: 3.96%, N: 9.17%; found: C: 65.81%, H: 3.94%, N: 9.09%.

Hexakis{[(4-(chloro)benzamide)methaneylidene]azaneylylidene}triazaphosphazene, 5h. Intermediate **4h** (1.40 g, 5.69 mmol) was used in the reaction. Yield: 1.25 g (68.89%), mp: 272.5–275.8 °C, orange powder. FTIR (cm⁻¹): 3360 (N–H stretching), 1695 (C=O stretching), 1644 (C=N stretching), 1601 (aromatic C=C stretching), 1254 (C–O stretching), 1189 (P=N stretching), 1172 (C–N stretching), 1014 (P–O–C stretching), 819 (C–Cl bending). ¹H-NMR (500 MHz, DMSO-d₆) δ, ppm: 8.44 (s, 1H), 7.86 (d, *J* = 10.0 Hz, 2H), 7.77 (d, *J* = 10.0 Hz, 2H), 7.41 (d, *J* = 5.0 Hz, 2H), 7.39 (d, *J* = 10.0 Hz, 2H), 7.14 (d, *J* = 10.0 Hz, 2H), 6.79 (d, *J* = 10.0 Hz, 2H). ¹³C-NMR (125 MHz, DMSO-d₆) δ, ppm: 167.36, 156.69, 156.48, 142.59, 138.31, 136.02, 135.30, 131.48, 130.20, 130.05, 129.18, 129.00, 123.00, 116.27. ³¹P-NMR (500 MHz, DMSO-d₆) δ, ppm: 8.53 (s, 1P). CHN elemental analysis: calculated for C₁₂₀H₈₄Cl₆N₁₅O₁₂P₃: C: 64.53%, H: 3.79%, N: 9.42%; found: C: 64.13%, H: 3.77%, N: 9.38%.

Hexakis{[(4-(nitro)benzamide)methaneylidene]azaneylylidene}triazaphosphazene, 5i. Intermediate **1** (1.50 g, 1.74 mmol) and intermediate **4i** (3.13 g, 0.012 mol) were used in the reaction. Yield: 2.23 g (71.15%), mp: 280.1–283.3 °C, yellow powder. FTIR (cm⁻¹): 3367 (N–H stretching), 1691 (C=O stretching), 1641 (C=N stretching), 1598 (aromatic C=C stretching), 1252 (C–O stretching), 1187 (P=N stretching), 1173 (C–N stretching), 1019 (P–O–C stretching). ¹H-NMR (500 MHz, DMSO-d₆) δ, ppm: 9.81 (s, 1H), 8.66 (s, 1H), 8.23 (d, *J* = 10.0 Hz, 2H), 8.04 (d, *J* = 10.0 Hz, 2H), 7.26 (d, *J* = 10.0 Hz, 2H), 6.82 (d, *J* = 10.0 Hz, 2H), 6.51 (d, *J* = 10.0 Hz, 2H), 6.46 (d, *J* = 10.0 Hz, 2H). ¹³C-NMR (125 MHz, DMSO-d₆) δ, ppm: 157.63, 155.02, 148.82, 148.71, 142.42, 142.05, 140.85, 129.47, 124.29, 123.79, 123.56, 116.32, 116.06, 116.01. ³¹P-NMR (500 MHz, DMSO-d₆) δ, ppm: 8.54 (s, 1P). CHN elemental analysis: calculated for C₁₂₀H₈₄N₂₁O₂₄P₃: C: 62.75%, H: 3.69%, N: 12.81%; found: C: 62.33%, H: 3.65%, N: 12.69%.

Synthesis of hexakis{[(4-(amino)benzamide)methaneylidene]azaneylylidene}triazaphosphazene, 5j. Compound **5j** was synthesized according to the method reported by Deyan *et al.* (2015) with some modifications.⁴⁸ A solution of compound **5i** (1.20 g, 0.52 mmol) in 20 mL hot ethanol and a solution of sodium sulphide hydrate, Na₂S·9H₂O (0.33 g, 4.18 mmol) in 10 mL ethanol and 10 mL water were mixed in a 100 mL round bottom flask. The mixture was refluxed for 7 hours. The reaction

progress was monitored using TLC. Upon completion, the mixture was cooled in an ice bath and the precipitate formed was filtered, washed with cold ethanol and dried overnight. Yield: 0.71 g (64.20%), mp: 296.4–298.7 °C, light brown powder. FTIR (cm⁻¹): 3360 (N–H amide stretching), 3416 and 3207 (N–H amine stretching), 1690 (C=O stretching), 1645 (C=N stretching), 1591 (aromatic C=C stretching), 1254 (C–O stretching), 1196 (P=N stretching), 1172 (C–N stretching), 1013 (P–O–C stretching). ¹H-NMR (500 MHz, DMSO-d₆) δ, ppm: 8.68 (s, 1H), 8.25 (d, *J* = 5.0 Hz, 2H), 8.06 (d, *J* = 5.0 Hz, 2H), 7.27 (d, *J* = 10.0 Hz, 2H), 6.99 (d, *J* = 5.0 Hz, 2H), 6.84 (d, *J* = 5.0 Hz, 2H), 6.56 (d, *J* = 10.0 Hz, 2H), 5.16 (s, 2H). ¹³C-NMR (125 MHz, DMSO-d₆) δ, ppm: 157.67, 155.00, 148.73, 147.96, 142.47, 142.07, 129.64, 129.47, 128.94, 124.29, 123.56, 119.45, 116.32, 115.76. ³¹P-NMR (500 MHz, DMSO-d₆) δ, ppm: 8.55 (s, 1P). CHN elemental analysis: calculated for C₁₂₀H₉₆N₂₁O₁₂P₃: C: 68.08%, H: 4.57%, N: 13.89%; found: C: 67.77%, H: 4.59%, N: 13.79%.

4. Conclusion

All the intermediates and hexasubstituted cyclotriphosphazene compounds were successfully synthesized and characterized. POM has been used to determine the mesophase behaviour of these compounds and the results showed that only compounds **5a–e** with alkoxy chains have liquid crystal properties. However, other compounds **5f–j** were found to be non-mesogenic with no liquid crystal behaviour. The presence of the amide linking unit caused compounds **5f–j** with small substituent such as hydroxy, carboxy, chloro, nitro, and amino have high melting temperature and liquid crystal behaviour cannot be induced although the Schiff base provide linearity and thermal stability in the molecules. The XRD data of compound **5c** confirmed the formation of SmA phase. The homeotropic alignment was occurred and suggested that the side arms were aligned three up and three down. Further study on the fire retardancy of final compounds was done using LOI testing. All the compounds gave excellent results and compound **5i** showed the highest LOI value with 28.53%. The effect of electron withdrawing of nitro group play an important role for the compound to have high fire retardant value as this nitro group can induced the P–N synergistic effect.

Conflicts of interest

The authors declare no conflict of interest.

Acknowledgements

The authors would like to thank the Universiti Malaysia Sabah (UMS) for Grant No. SGA0037-2019 and Universiti Sains Malaysia (USM) for RUI (USM) Grant No. 1001/PKIMIA/811332.

References

- 1 H. R. Allcock and R. L. Kugel, *J. Am. Chem. Soc.*, 1965, **87**, 4216–4217.
- 2 H. R. Allcock, *Chem. Rev.*, 1972, **72**, 315–356.



3 K. Moriya, T. Suzuki, S. Yano and M. Kajiwara, *Liq. Cryst.*, 1995, **19**, 711–713.

4 H. R. Allcock, *Phosphorus, Sulfur Silicon Relat. Elem.*, 2004, **179**, 661–671.

5 J. Barberá, J. Jiménez, A. Laguna, L. Oriol, S. Pérez and J. L. Serrano, *Chem. Mater.*, 2006, **18**, 5437–5445.

6 J. M. Khurana, S. Chauhan and G. Bansal, *Monatsh. Chem.*, 2004, **135**, 83–87.

7 Z. Hussain, F. Qazi, M. I. Ahmed, A. Usman, A. Riaz and A. D. Abbasi, *Biosens. Bioelectron.*, 2016, **85**, 110–127.

8 S. Singh and D. Dunmur, *Liquid crystals: Fundamentals*, World Scientific, 2002, pp. 1–3.

9 P. J. Collings and M. Hird, *Introduction to Liquid Crystal Chemistry and Physic*, Taylor & Francis, MIT Press, London, 1997.

10 P. J. Collings, *Liquid Crystals: Nature's Delicate Phase of Matter*, Princeton Univ. Press, New Jersey, 2nd edn, 2002, p. 204.

11 C. Kim and H. R. Allcock, *Macromolecules*, 1987, **20**, 1726–1727.

12 K. Moriya, H. Mizusaki, M. Kato, T. Suzuki, S. Yano, M. Kajiwara and K. Tashiro, *Chem. Mater.*, 1997, **9**, 255–263.

13 K. Moriya, T. Suzuki, H. Mizusaki, S. Yano and M. Kajiwara, *Chem. Lett.*, 1997, **26**, 1001–1002.

14 D. Frenkel and B. M. Mulder, *Mol. Phys.*, 1985, **55**, 1171–1192.

15 Z. Jamain, M. Khairuddean, N. N. Zulbaharen and T. K. Chung, *Malaysian Journal of Chemistry*, 2019, **21**, 73–85.

16 K. Václav, H. Martin, S. Jiří, N. Vladimíra and P. Damian, *Liq. Cryst.*, 2012, **39**, 943–955.

17 G. W. Gray, *Molecular structure and the properties of liquid crystals*, Academic Press, London, 1962.

18 L. Jiménez, A. Laguna, A. M. Molter, J. L. Serrano, J. Barberá and L. Oriol, *Chem.-Eur. J.*, 2011, **17**, 1029–1039.

19 Q. He, H. Dai, X. Tan, X. Cheng, F. Liu and C. Tscherske, *J. Mater. Chem. C*, 2013, **1**, 7148–7154.

20 Y. Jae Shin, Y. Rok Ham, S. H. Kim, D. H. Lee, S. B. Kim, C. S. Park, Y. M. Yoo, J. G. Kim, S. H. Kwon and J. S. Shin, *J. Ind. Eng. Chem.*, 2010, **16**, 364–367.

21 Y. L. Liu, Y. C. Chiu and T. Y. Chen, *Polym. Int.*, 2003, **52**, 1256–1261.

22 K. Faghihi and M. Hagibeygi, *Turk. J. Chem.*, 2007, **31**, 65–73.

23 X. Zhang, Y. Zhong and Z. Mao, *Polym. Degrad. Stab.*, 2012, **97**, 1504–1510.

24 Y. Rong, H. Wentian, X. Liang, S. Yan and L. Jinchun, *Polym. Degrad. Stab.*, 2015, **122**, 102–109.

25 Y. Rong, W. Bo, H. Xiaofeng, M. Binbin and L. Jinchun, *Polym. Degrad. Stab.*, 2017, **144**, 62–69.

26 K. Moriya, T. Masuda, T. Suzuki, S. Yano and M. Kajiwara, *Mol. Cryst. Liq. Cryst.*, 2006, **318**, 267–277.

27 S. Ahuja and N. Jespersen, *Modern Instrumental Analysis*, Elsevier Science, 2006.

28 D. Pociecha, D. Kardas, E. Gorecka, J. Szydłowska, J. Mieczkowski and D. Guillon, *J. Mater. Chem.*, 2003, **13**, 34–37.

29 B. Y. Zhang, Y. G. Jia, D. S. Yao and X. W. Dong, *Liq. Cryst.*, 2004, **31**, 339–345.

30 D. Davarci, *CBU J. Sci.*, 2016, **12**, 535–542.

31 M. Hird, J. W. Goodby, N. Gough and K. J. Toyne, *J. Mater. Chem.*, 2001, **11**, 2732–2742.

32 Z. Jamain, M. Khairuddean and S. A. Saidin, *J. Mol. Struct.*, 2019, **1186**, 293–302.

33 Z. Jamain, M. Khairuddean and T. Guan-Seng, *Int. J. Mol. Sci.*, 2020, **21**, 4267.

34 E. L. Heeley, D. J. Hughes, Y. El Aziz, I. Williamson, P. G. Taylor and A. R. Bassindale, *Phys. Chem. Chem. Phys.*, 2013, **15**, 5518–5529.

35 H. Kelker and R. Hatz, *Handbook of liquid crystals*, Verlag Chemie, Weinheim, Germany, Deerfield Beach, Florida, USA, 1980.

36 Z. Jamain, M. Khairuddean and T. Guan-Seng, *Molecules*, 2020, **25**, 2122.

37 J. A. Uhood, E. G. Tarik and H. R. Howraa, *Molecules*, 2010, **15**, 5620–5628.

38 Z. Galewski and H. J. Coles, *J. Mol. Liq.*, 1999, **79**, 77–87.

39 H. S. El-Wahab, *Pigm. Resin Technol.*, 2015, **44**, 101–110.

40 S. Zahra, J. Nasrin and S. Shahla, *Carbohydr. Polym.*, 2015, **118**, 183–198.

41 W. De-Yi, *Novel Fire Retardant Polymers and Composite Materials*, Woodhead Publishing Series in Composites Science and Engineering: Number 73, 2017.

42 K. A. Salmeia, S. Gaan and G. Malucelli, *Polymers*, 2016, **8**, 319–355.

43 H. Chun-Chieh, C. Yu-Chaing, C. San-Yuan and L. Hong-Cheu, *RSC Adv.*, 2016, **6**, 32319–32327.

44 A. H. Davidson, S. J. Davies and D. F. C. Moffat, *PCT Int. Appl.*, 2006, 2006117552.

45 Z. Shaoyu and X. Jiangbing, Faming Zhuanli Shenqing, CN102618062, 2012.

46 A. P. Avdeenko and I. L. Marchenko, *Russ. J. Org. Chem.*, 2001, **37**, 822–829.

47 G. Fareed, M. A. Versiani, N. Afza, N. Fareed, M. A. Kalhoro, S. Yasmeen and M. A. Anwar, *J. Chem. Soc. Pak.*, 2013, **35**, 427–431.

48 Z. Deyan, W. Yangyang, J. Jiong, Y. Wenzhu, Q. Baofeng, L. Xia and S. Xuan, *ChemComm*, 2015, **51**, 10656–10659.

